Impact of grid refinement on SRS LES calculation

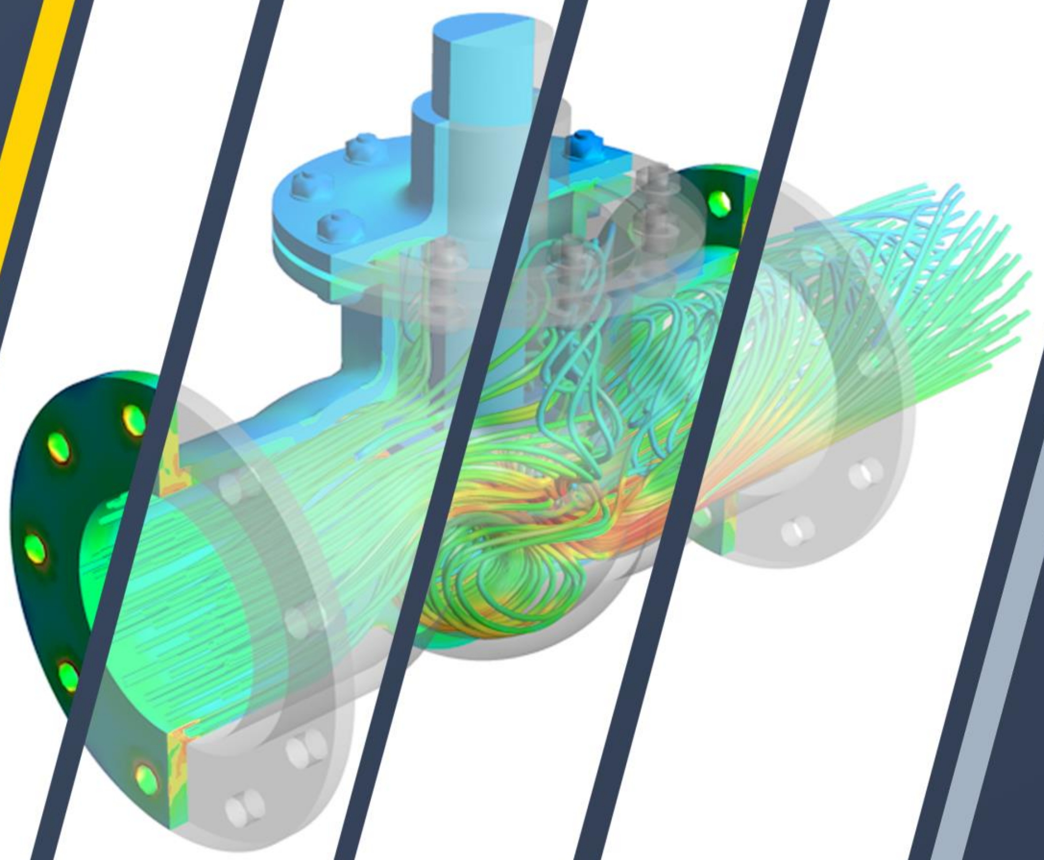

V.1.1
J. Lavedrine
ANSYS France

08/2019

Index

Index

1. **Description**
   1. Brief reminder on LES principles
   2. Impact of grid refinement in LES?
2. Solution
   1. Description of computational grids and setup
   2. Computational cost
   3. Visualization of flow structures
   4. Time-averaged profiles and grid-independence
   5. Assessment of tke spectra
   6. Scatter-plot of velocity (instantaneous vs mean) inside domain
3. Summary
   1. Observations on grid refinement for LES
   2. Some words on RANS and LES

1.1 Definition of spatial filter for LES

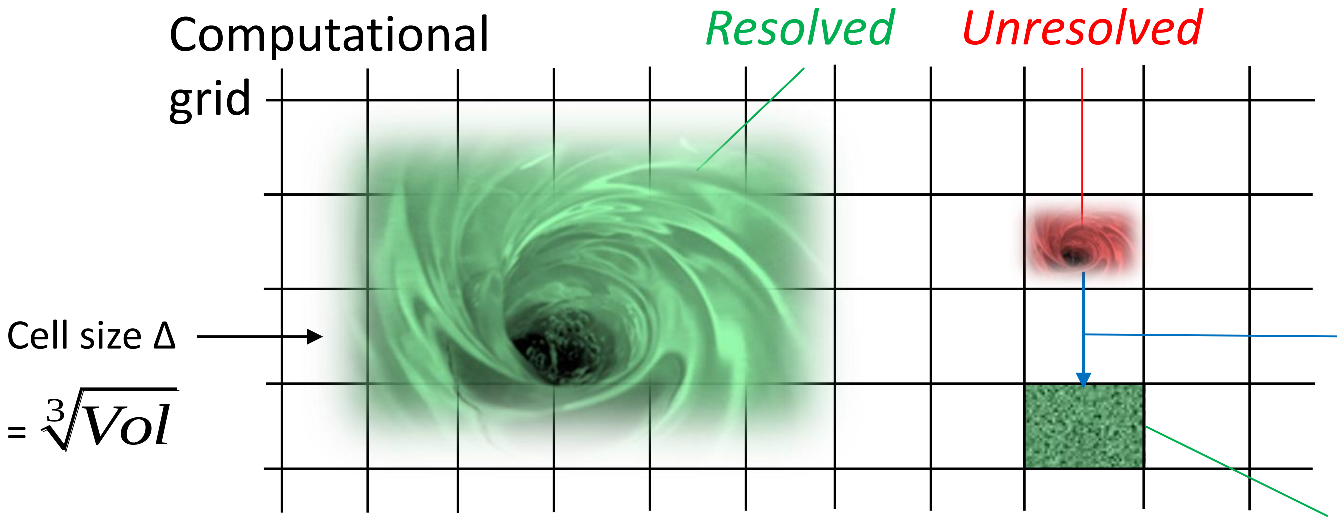

A homogeneous filter is considered here!

Small vortices are assumed more isotropic than larger ones.
→ Easier to model!

The LES filter function G can be defined both spatially and temporally:

$$\hat{\varphi}(\mathbf{x},t) = \iiint_{X} \int_{t'} \varphi(X,t') \cdot \boxed{G(\mathbf{x}-X,t-t')} d^3X dt'$$

This filter can be applied to the instantaneous velocity field:

$$u(x,t) = \hat{u}(x,t) + u''(x,t)$$

Instantaneous | Filtered Resolved | **S**ub-**G**rid **S**cale (**SGS**) Residual

After applying this filter to NS equations, unclosed terms appear which are usually modeled using an eddy viscosity assumption.
This eddy viscosity is related to local grid sizing, entailing that a coarser grid will produce higher eddy dissipation through SGS modeling.

1.1 LES rationale

Main ideas of LES:

- Resolving the turbulence spectrum up to dissipative scales (Kolmogorov scales) requires huge computational resources in most cases (moderate to large Reynolds numbers).
- Energy has to be dissipated from the spectrum at ***grid limit***.
- LES eddy viscosity (from SGS model in fact) provides the required ***damping***.
- LES does not *explicitly* model the small scales.

→ it just needs to ***dissipate*** them at a relevant rate!

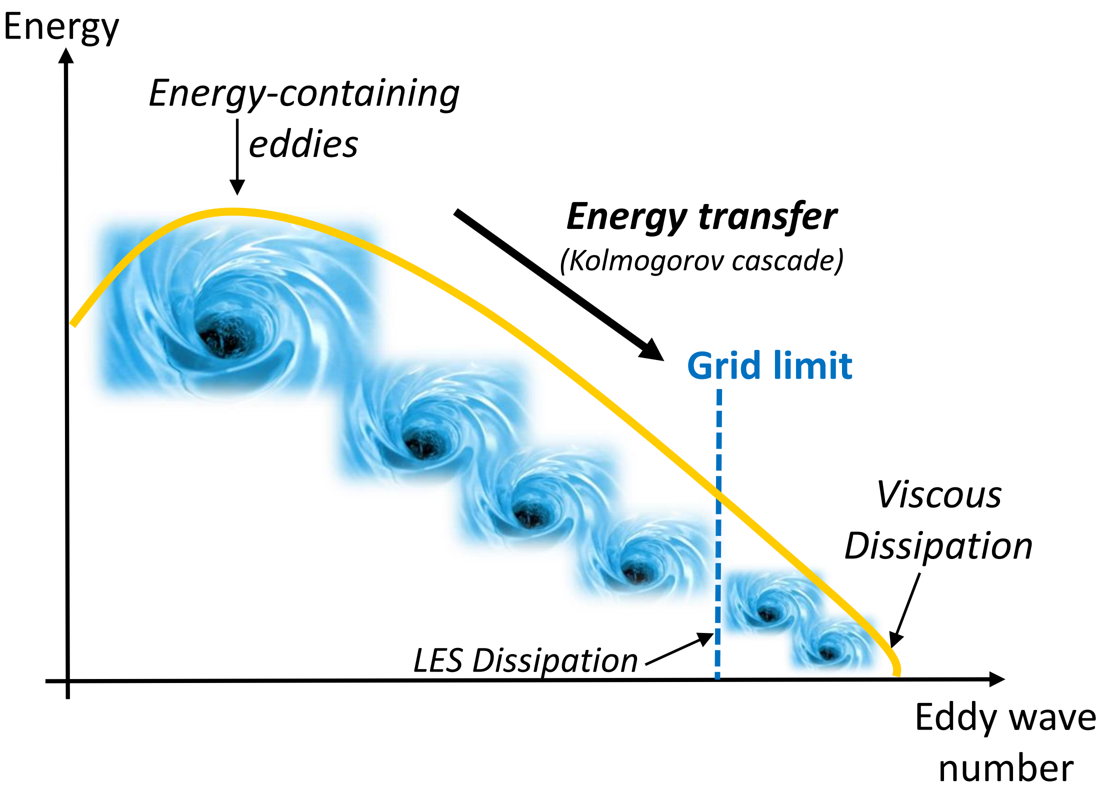

→ In LES, every eddy that is deemed relevant to capture proper flow dynamics has to be properly resolved!

1.2 Can you provide some insight into the impact of grid refinement over LES results?

You can find valuable solutions on ANSYS customer portal to obtain guidelines on how to prepare a relevant grid for SRS calculations such as LES. Please take a look at addenda for additional solutions on this topic as well as general references on LES.

In this solution, purpose is more to show you the impact of different cell sizes over LES results in the core flow of a tee mixing region. Refining mesh is simply done through a refining factor of 2 in all 3 directions using adaptation technique in ANSYS Fluent. Such refinement strategy is applied 3 times, which sums up to 4 grids in total.

An assessment of computational costs is also provided for the different grids.

Index

1. Description
   1. Brief reminder on LES principles
   2. Impact of grid refinement in LES?

2. **Solution**
   1. Description of computational grids and setup
   2. Computational cost
   3. Visualization of instantaneous flow structures
   4. Time-averaged profiles and grid-independence
   5. Assessment of tke spectra
   6. Scatter-plot of velocity (instantaneous vs mean) inside domain

3. Conclusions
   1. Advice on grid refinement for LES
   2. Some words on RANS and LES

2.1 Description of computational grids

Turbulent flow in a mixing tee

Air at ambiant conditions

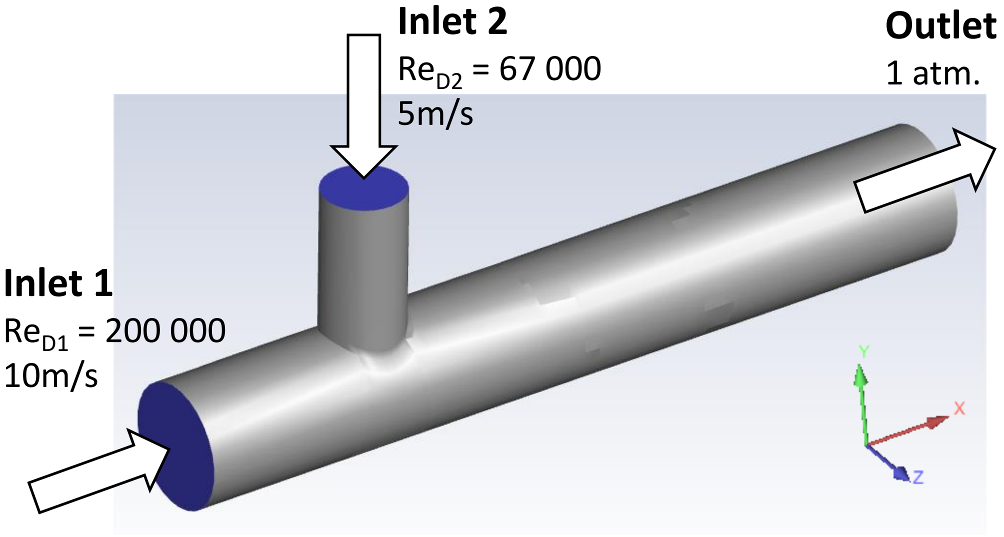

- Near-wall mesh is refined through dedicated bunching (geometric growth rate).
- Global refinement is performed using adaptation in ANSYS Fluent, allowing one to get a perfect refinement ratio of 2 per adaptation step.

3D Refinement factor of 2^3 between 2 consecutive cases

Grid no.	1	2	3	4
Cell count	~ 23 000	~ 183 000	~ $1.5*10^6$	~ $12.0*10^6$
		* 2^3	* 2^3	* 2^3
Cell type	Hexahedra*			
Min cell size [m]	0.010	0.005	0.0024	0.0012
		* 0.5	* 0.5	* 0.5
Max cell size [m]	0.029	0.015	0.007	0.0035
Min Orthogonal quality	~0.6			
Max aspect ratio	~20			

*Blocking approach with traversing O-grid under ICEM CFD R2019 R1

2.1 Mesh density of computational grids (1)

Grid 1
23k cells

Grid 2
183k cells

Grid 3
1.5M cells

Grid 4
12M cells

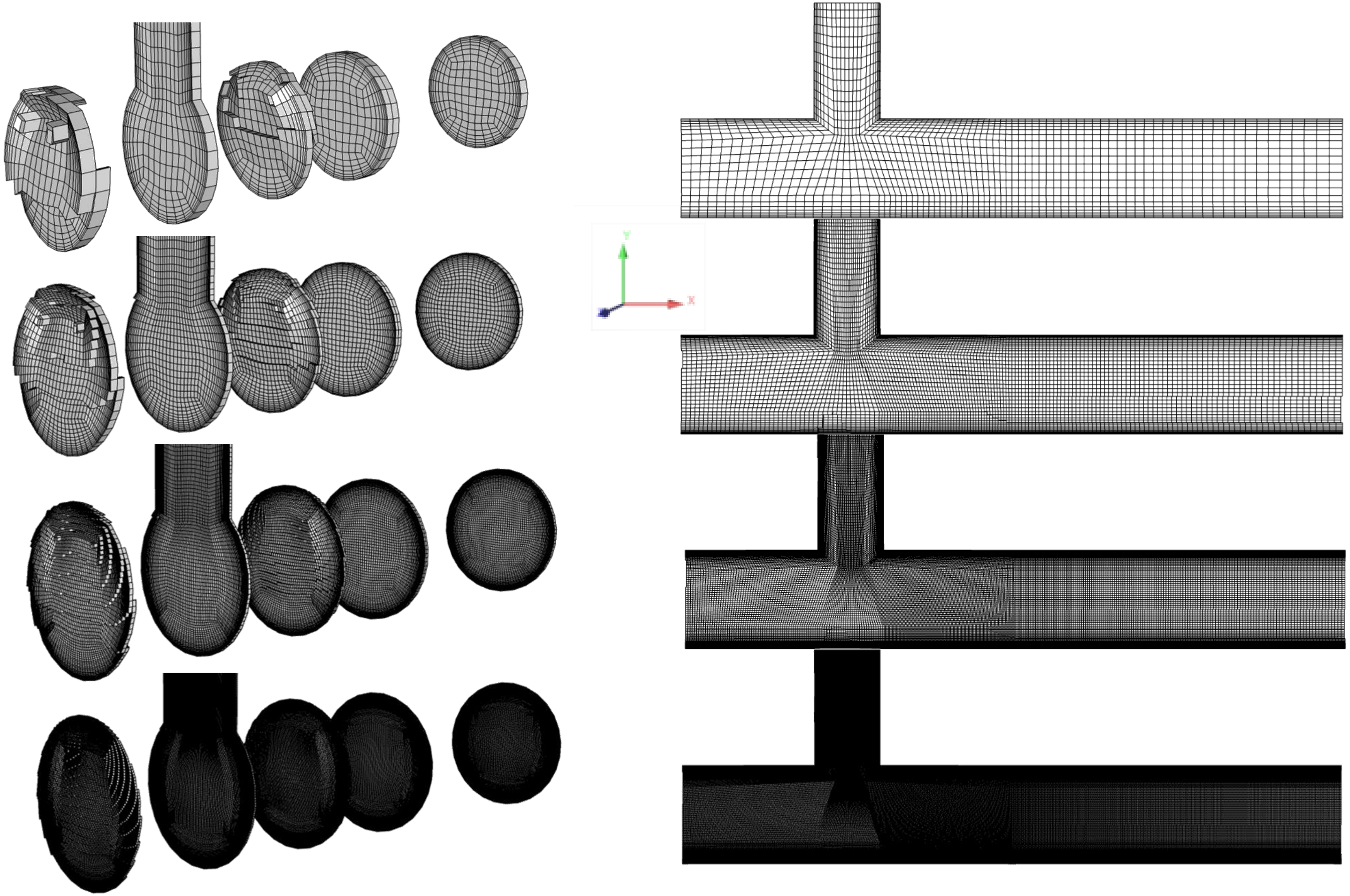

2.1 Mesh density of computational grids (2)

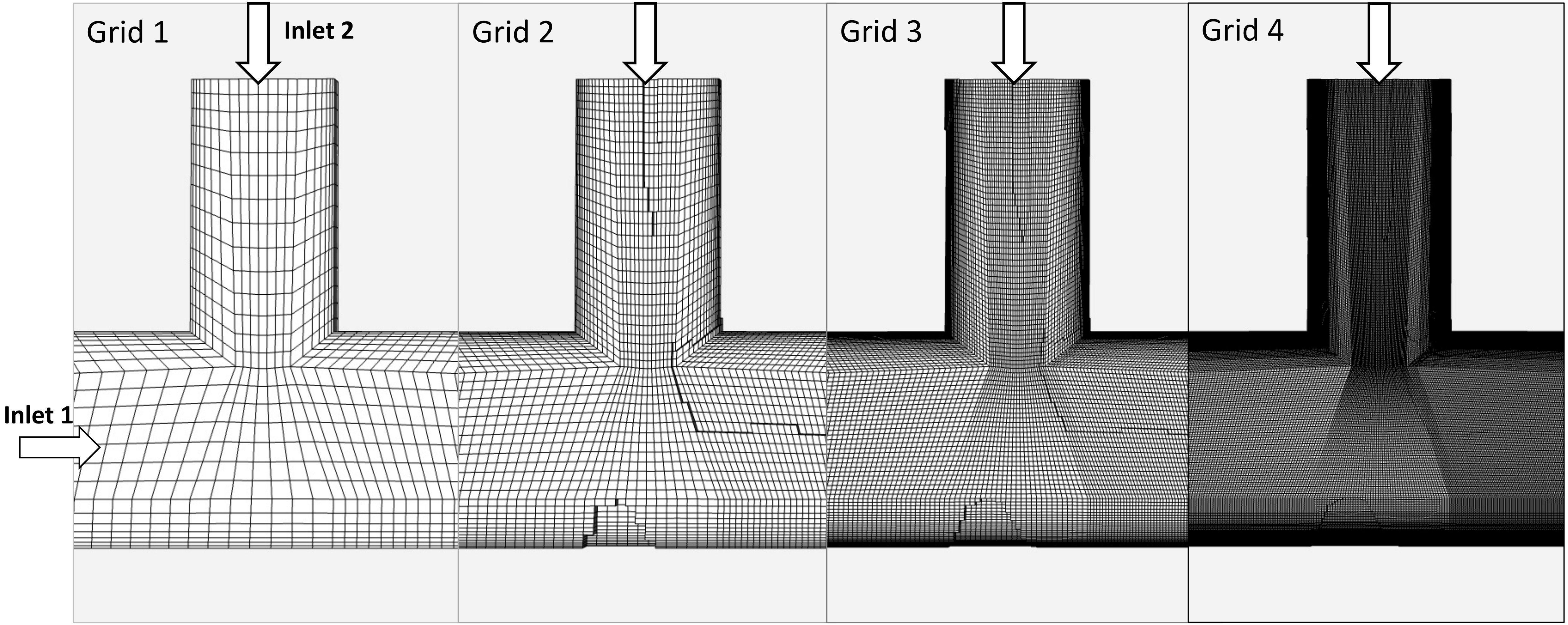

2.1 Case setup

CFD Tool: **ANSYS Fluent R2019 R1**

- 3D unsteady pressure-based solver
- SGS model: Smagorinsky standard (C_S = 0.1)
- Air with constant properties at ambiant conditions (1 atm, 300K)

- Inlet with fully developped velocity profiles*
- Vortex method at both inlets
- Outlet at atmospheric pressure
- Initialization with potential flow
- Before collecting statistics, preliminary transient calculation is performed to properly develop turbulent flow

- Coupled pressure/velocity algorithm
- Gradient calculation: Least-Square Cell-Based
- Pressure: Second order
- Momentum: Bounded Central-Differencing
- Time: Bounded Second-Order Implicit

*obtained from preliminary calculations with periodic pipes

2.2 Case setup and computational cost

Calculation no.*	1		2		3		4
Total cell #	~ 23 000	*8	~ 183 000	*8	~ $1.5*10^{6}$	*8	~ $12.0*10^{6}$
Mean Y+ [-]	54.9		25.6		13.2		6.9
Vortices # at each inlet	75		250		800		999
Timestep size** [s]	$5.0*10^{-4}$		$2.0*10^{-4}$		$1.0*10^{-4}$		$5.0*10^{-5}$
Duration for statistics [s]	1.0		1.0		1.0		1.0
Number of timesteps [-]	2000		5000		10000		20000
Mean / Max CFL [-]	0.26 / 1.57		0.22 / 1.83		0.22 / 2.18		0.22 / 2.87
Number of cores	5	* 1	5	* 11	56	* 2	112
Peak of RAM [Gb]	0.6	* 2	1.2	* 12	15.0	* 5	71.7
Total CPU time [h]	0.5	* 12	6.0	* 2.5	16.0	* 7.5	120.0

*Case no. refers to the same grid no.

**10 sub-iterations per timestep are considered.

2.3 Visualization of instantaneous flow structures (1a)

Isosurface of Q criterion = $5*10^4\ s^{-2}$ colored by the instantaneous eddy viscosity ratio

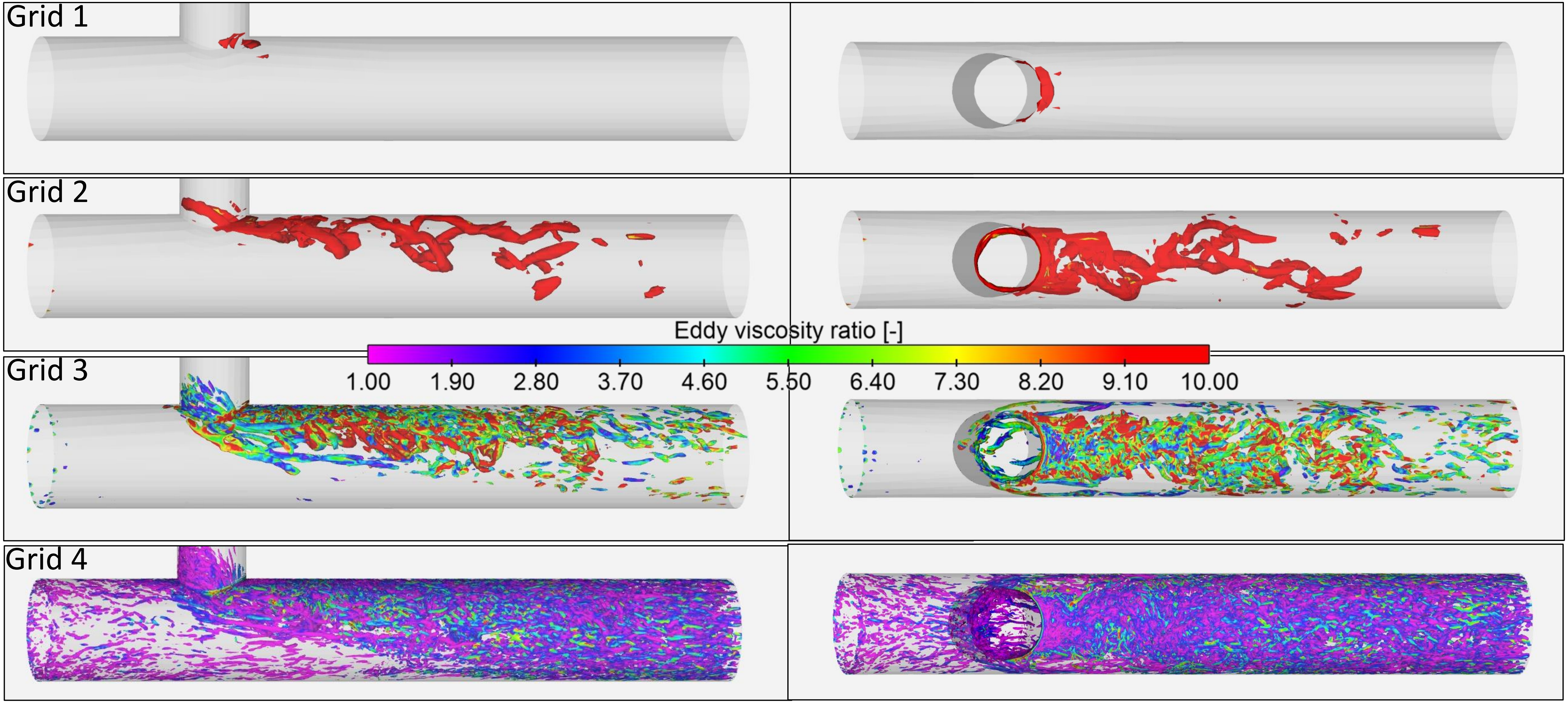

2.3 Visualization of instantaneous flow structures (1b)

Isosurface of Q criterion = $5*10^4$ s^{-2} colored by the instantaneous eddy viscosity ratio

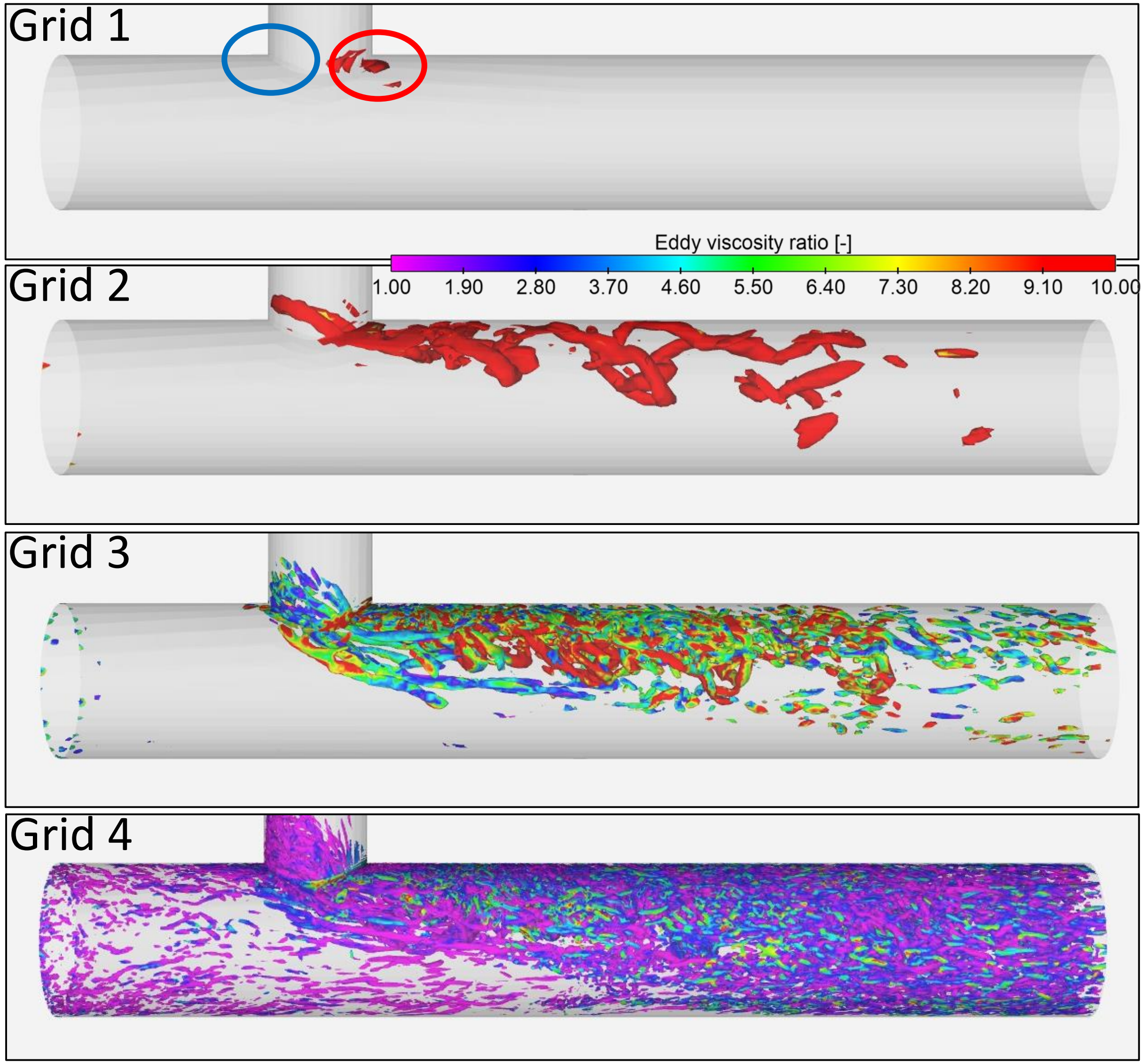

First obvious observation is that grid resolution strongly affects the eddies that are captured by the simulation.

Here, this effect is two-fold because on the finest grid 4, one captures more and finer eddies which also exhibit smaller eddy viscosity ratio. It clearly points to the fact that SGS eddy diffusion is smaller for grid 4 and allows more eddies to be transported if local turbulence generation is strong enough.

Calculation 1 shows very few strong eddies that are located primarily at the downstream wall intersection:

Calculation 2 and further refined calculations also capture eddies generated at upstream wall intersection:
→ Such flow feature is a strong trigger effect for turbulence and is completely missed in calculation 1 because fewer eddies concentrate flow turbulent kinetic energy!

2.3 Visualization of instantaneous flow structures (1c)

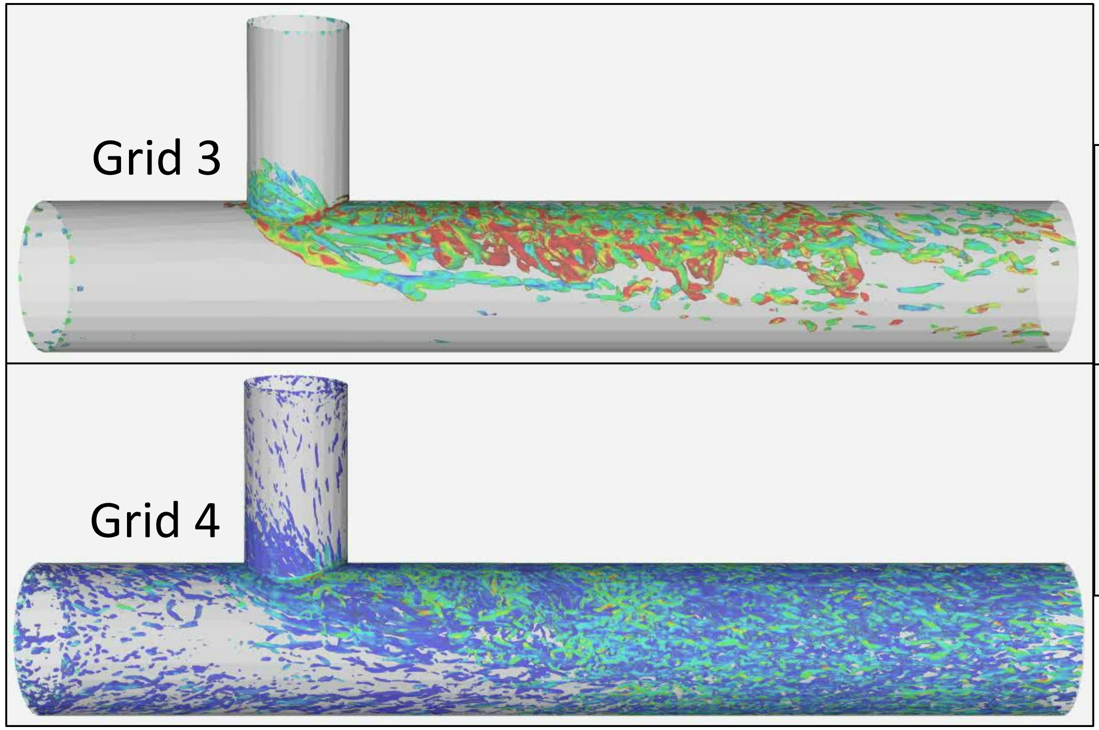

Isosurface of Q criterion = $5*10^4\ s^{-2}$ colored by the instantaneous eddy viscosity ratio

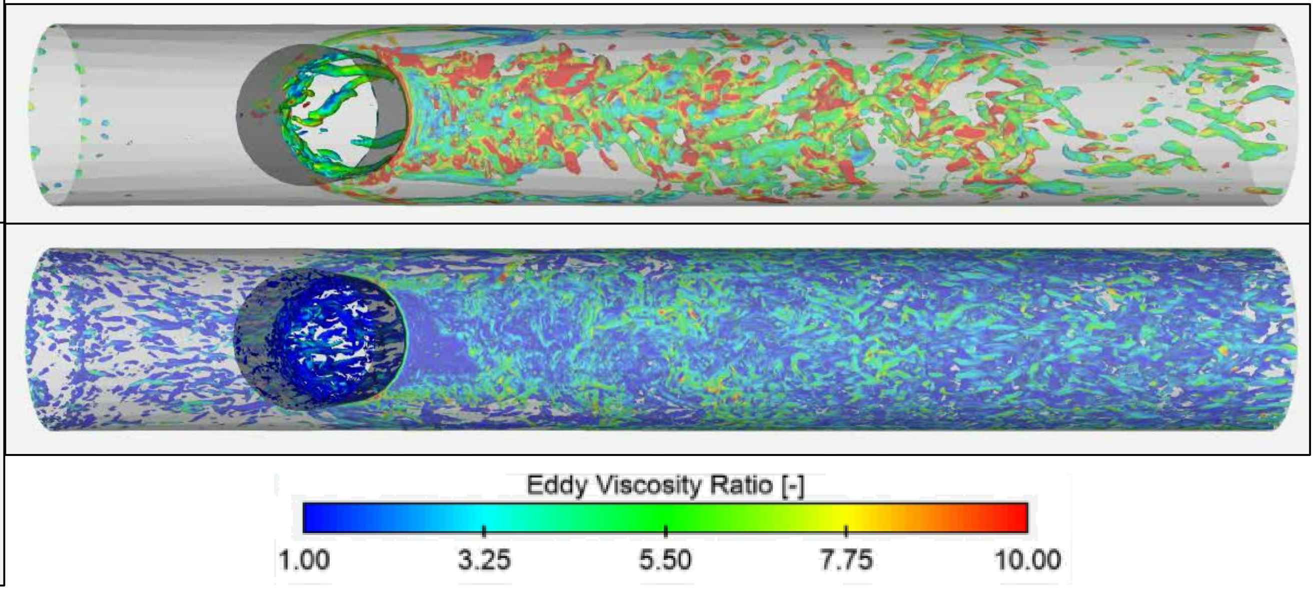

- Main turbulence generator is located at the junction between the pipes.
- Instantaneous motion of captured eddies shows strong anisotropic behaviour in both calculations, prefered flow direction being the tube main axis as expected.
- Calculation 4 limits values of eddy viscosity ratio well below 10 and sustains strong turbulent content up to the outlet, which is not the case for coarser grids.

Introducing vortices at inlets

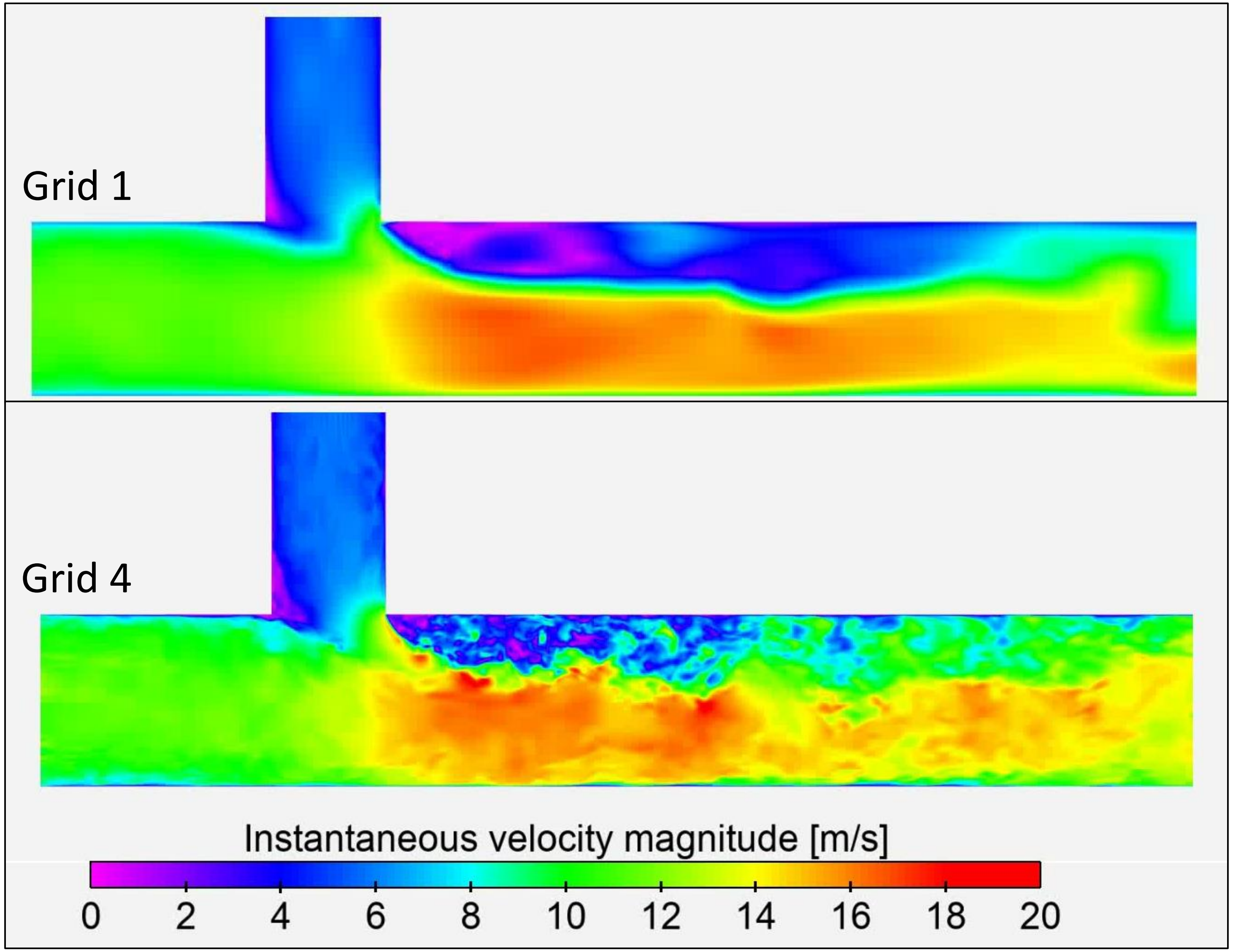

Mid-Z cut colored by the magnitude of instantaneous velocity.

Vortex method is introducing vortices from inlet and the number of vortices is linked to the number of faces of the inlet: best practice is usually to take Total face count / 4 as the number of vortices.

For grid 1, only 25 large vortices are injected per inlet.

For grid 4, mesh resolution allows user to reach maximum of 999 vortices per inlet. Thus, vortices injected can be smaller and their influence is still effective at tube junction.

2.3 Visualization of instantaneous flow structures (2)

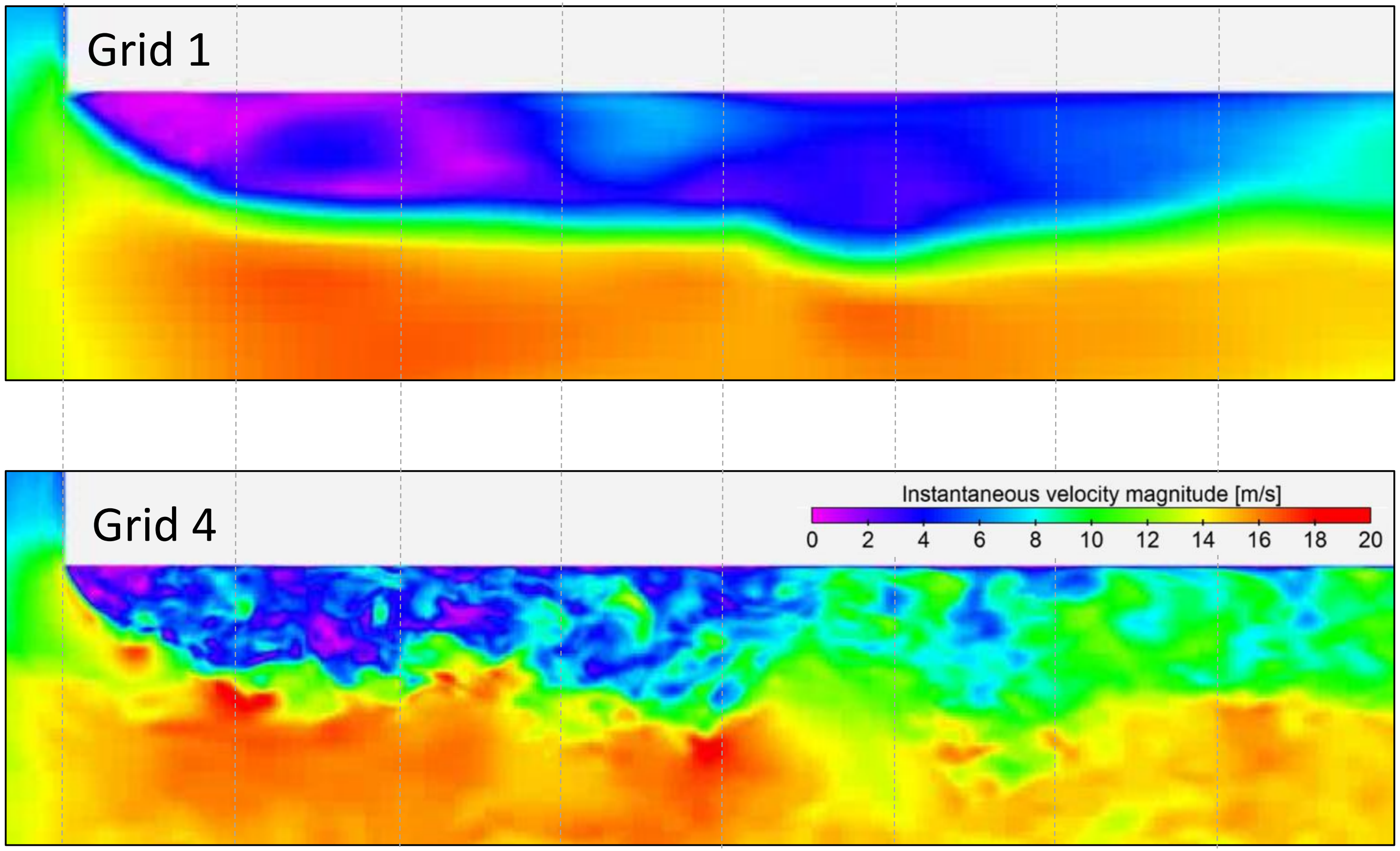

Mid-Z cut colored by the magnitude of instantaneous velocity. Detail in mixing region.

Another point is that calculation 1 captures a reduced number of large vortices that seem to move very slowly at the border of the recirculation bubble.

In calculation 4, vortices seem to move faster but in fact, the largest eddies captured move *at the same speed* as in calculation 1. Basically, smaller captured eddies are moving faster but on shorter distance before transfering energy to even smaller vortices.

Such process illustrates Kolmogorov cascade that is recovered on grid 4.

2.3 Visualization of instantaneous flow structures (3a)

Mid-Z cut colored by the magnitude of instantaneous strain rate.

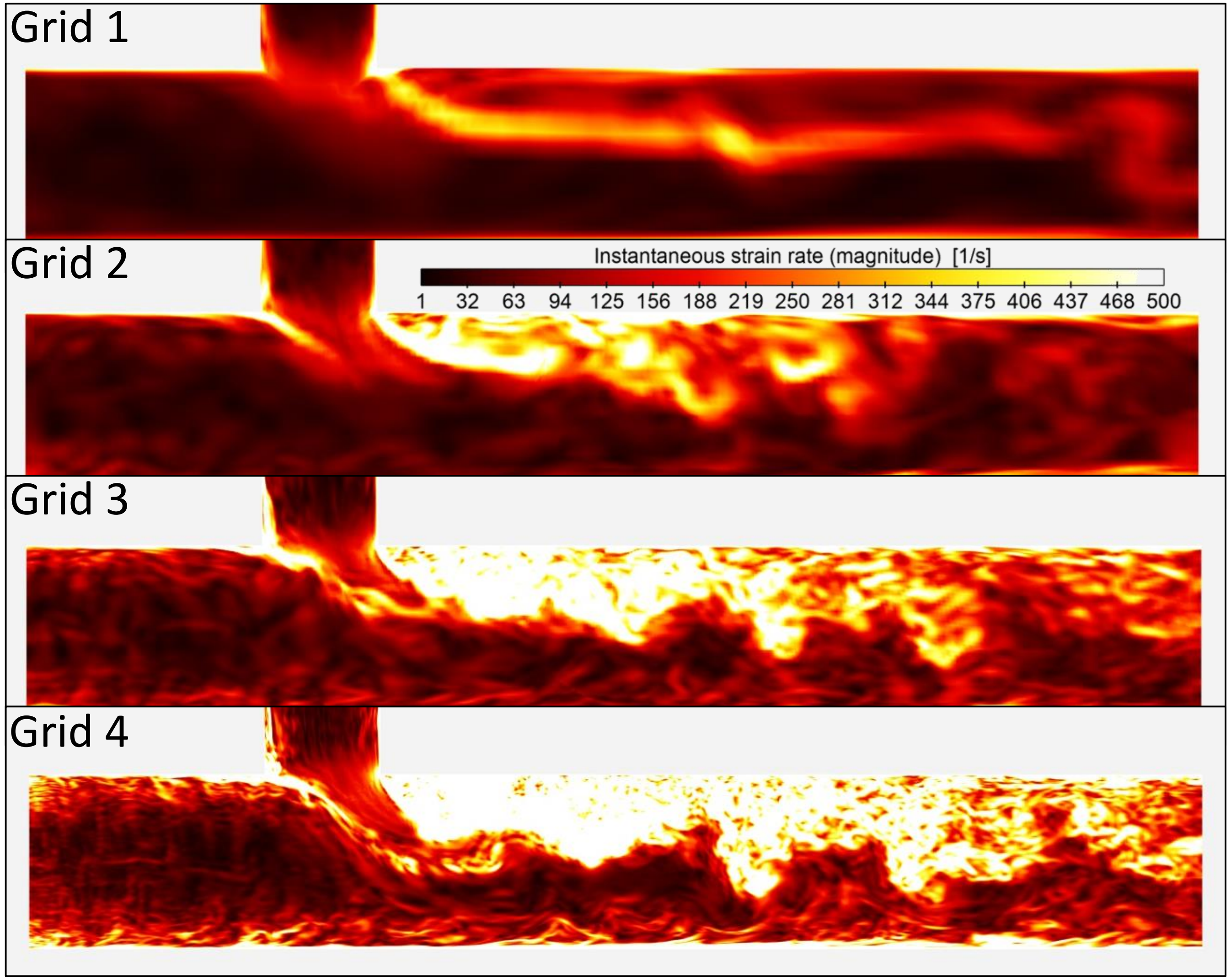

Smagorinsky model introduces a SGS viscosity which is simply related to the filtered strain rate through this expression:

$$\boxed{\nu_{SGS} = \left(C_S\hat{\Delta}\right)^2 |\hat{S}|}$$

Filtered strain rate is also related to filtered velocity gradients through:

$$\boxed{\hat{S} = \frac{1}{2}\left(\frac{\partial \hat{u}_i}{\partial x_j} + \frac{\partial \hat{u}_j}{\partial x_i}\right)}$$

So filtered strain rate remains a good marker of local eddy activity.

Refined mesh strongly decreases SGS turbulent viscosity, which allows the LES calculation to capture finer eddies and convect them further away without smearing them out. Also bear in mind that grid quality here reduces damping from numerics, which favors a convincing transport of eddies.

2.3 Visualization of instantaneous flow structures (3b)

Mid-Z cut colored by the magnitude of instantaneous resolved strain rate.

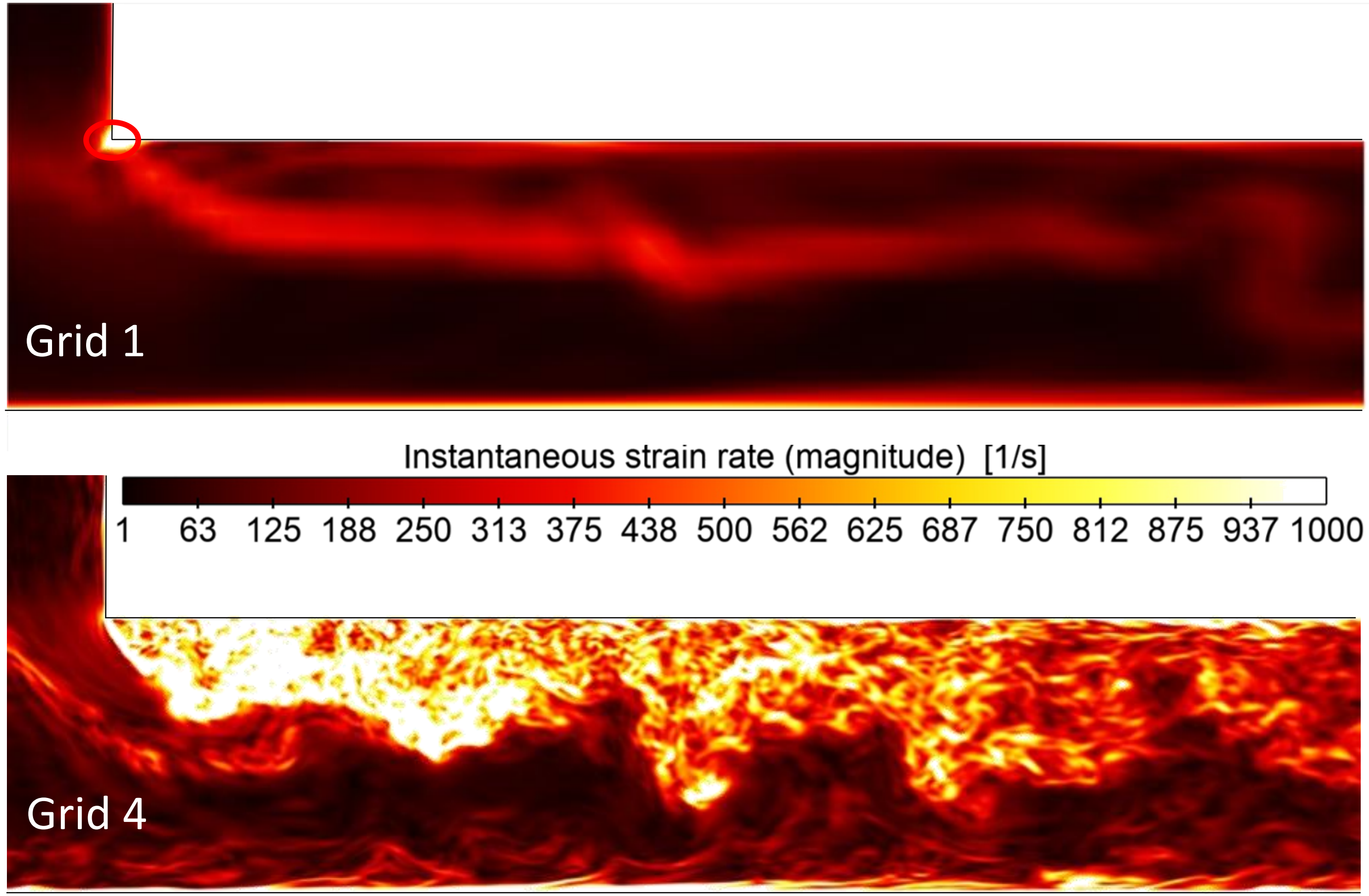

Spatial fields of instantaneous resolved strain rate show that :

1. Lower levels of strain rate are obtained for grid 1, except near the downstream corner: .
2. Even if resolved strain rate shows lower values for grid 1, eddy viscosity remains higher, confirming cell size Δ has strongest impact on eddy viscosity.
3. Calculation 1 detects local strain at corner but cannot transfer information further inside the domain: it is smeared out by coarse mesh.
4. Different eddy sizes can be distinguished on grid 4: large eddies convect packs of smaller eddies inside. Redistribution of kinetic energy between eddies operates here as stated on slide 17.
5. Decay of strain rate is much quicker on grid 1, SGS model + numerical diffusion from finite order spatial schemes both contribute to this effect.

2.3 Visualization of instantaneous flow structures (3c)

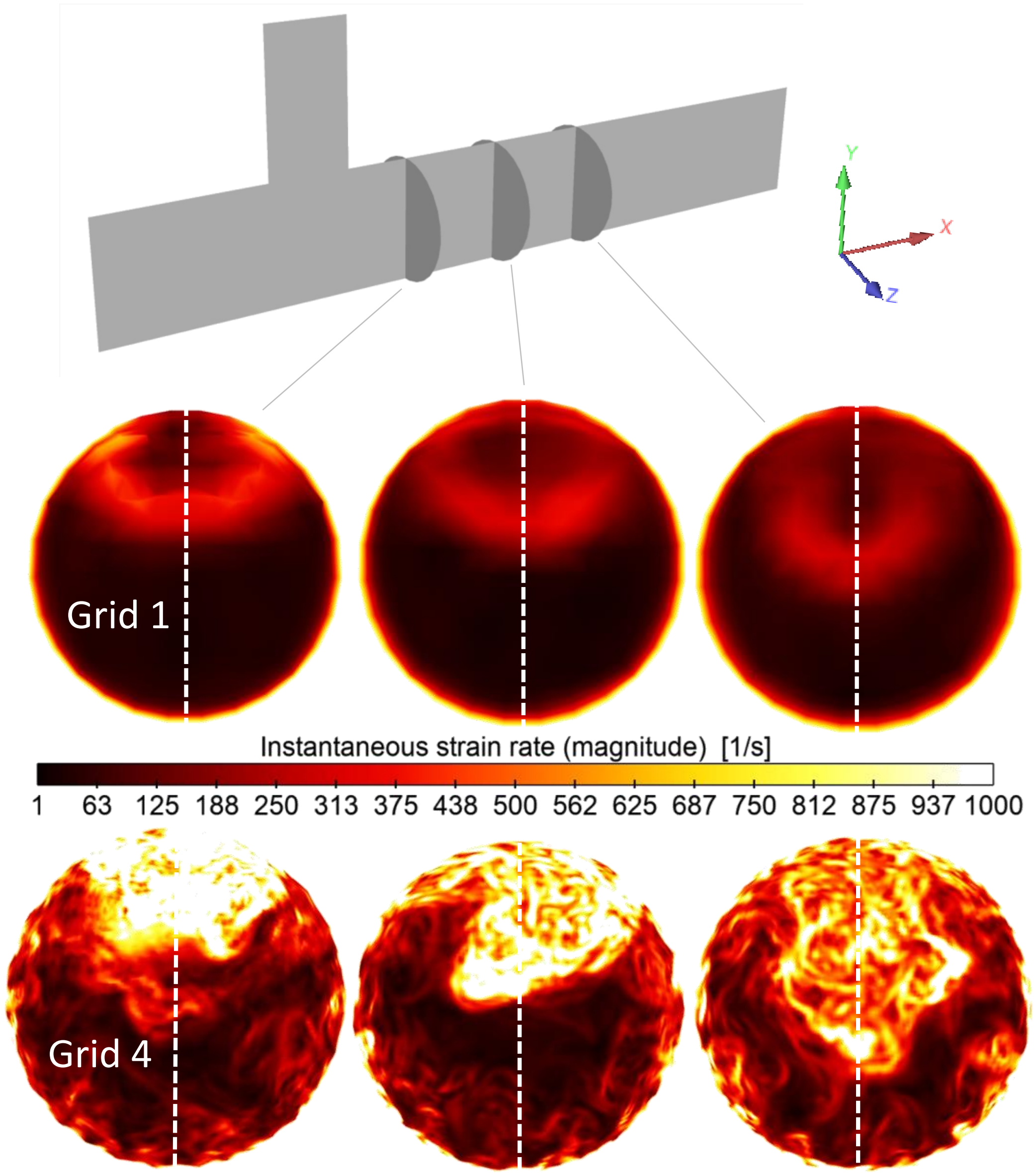

X cuts colored by the magnitude of instantaneous strain rate.

Calculation 1 introduces symetry along Z direction into the instantaneous spatial field of strain rate, which is not expected for the instantaneous flow. Only the time-averaged flow can be expected to be symetrical in such configuration.

The fact that such symetry is artificial and comes from the crude resolution of grid 1 is also confirmed by calculation 4. Instantaneous flow strain rate is then highly unsymetrical, particularly the motion of large eddies captured by grid 4.

Although LES can be carried out on coarse grids, simulation then relies more heavily on SGS modeling. Since Smagorinsky's model does not introduce anisotropy as a contribution from residual scales, it is not surprising that calculation 1 rapidly smoothes out any anisotropic behaviour from captured large scales.

2.4 Time-averaged Pope criterion (1)

Mid-Z cut colored by the time-averaged Pope criterion.
White line marks the recommended threshold M = 0.2.

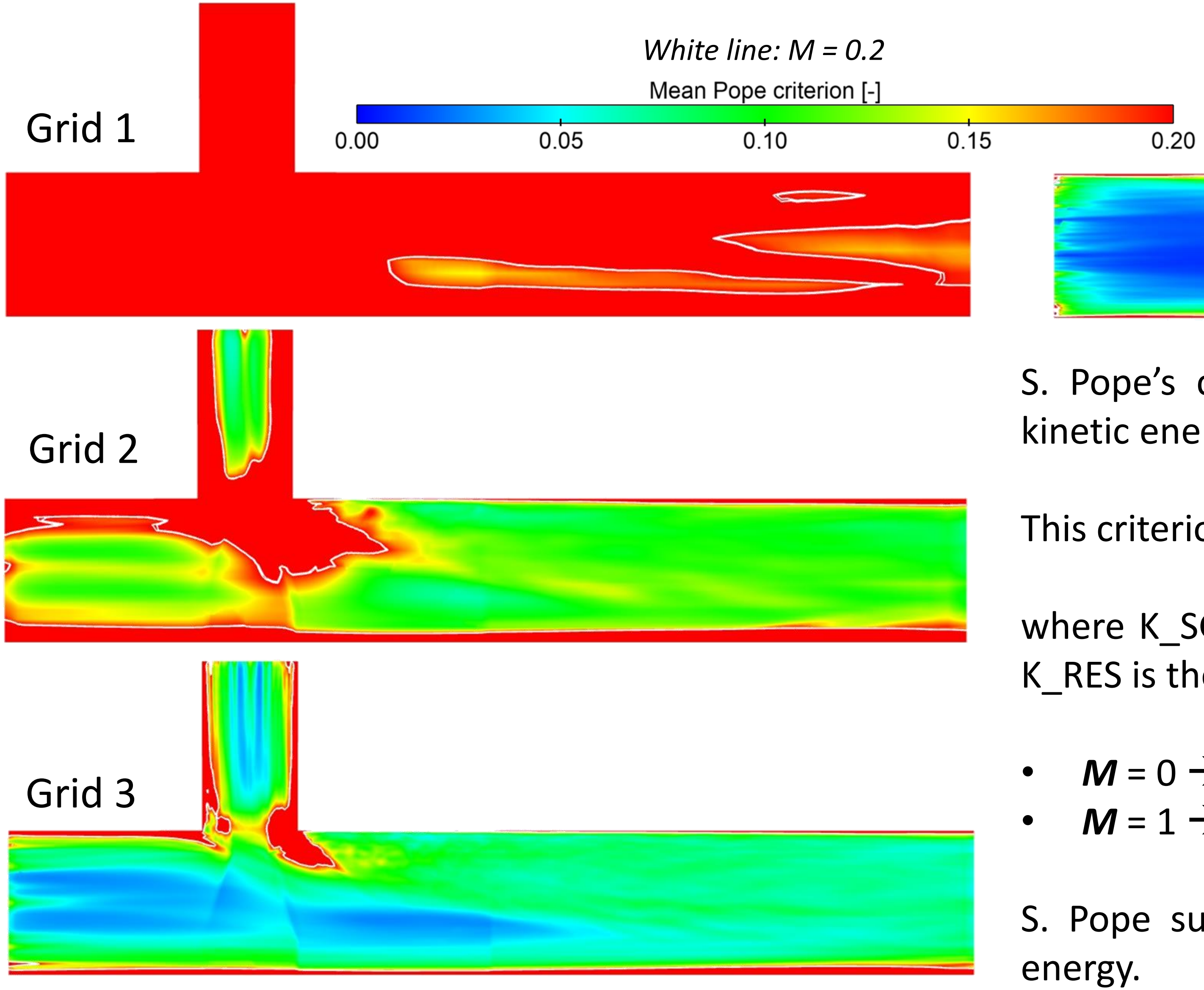

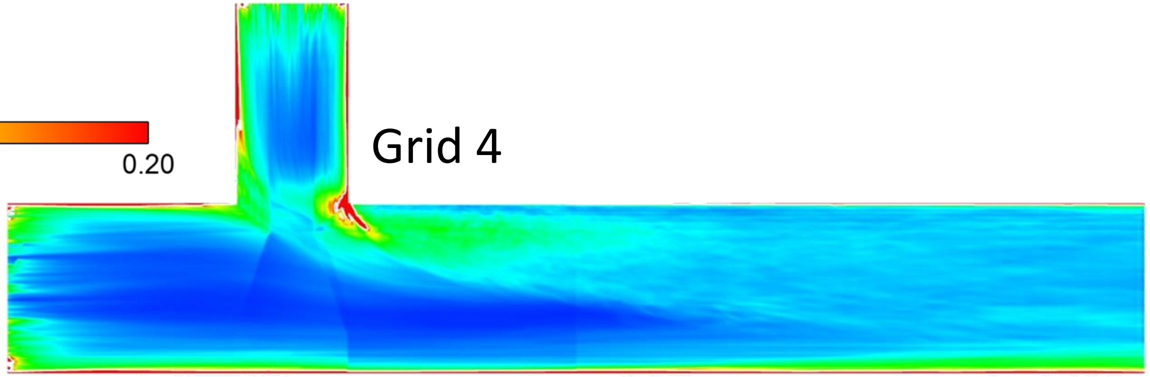

S. Pope's criterion provides a measure of the fraction of kinetic energy resolved by the LES simulation.

This criterion ***M*** reads: $\boldsymbol{M(x,t)} = \dfrac{\boldsymbol{K\_SGS(x,t)}}{\boldsymbol{K\_SGS(x,t) + K\_RES(x,t)}}$

where K_SGS is the turbulent kinetic of residual eddies and K_RES is the turbulent kinetic energy of the filtered eddies.

- ***M*** = 0 → Direct Numerical Simulation (DNS)
- ***M*** = 1 → Reynolds-Averaged Navier-Stokes (RANS)

S. Pope suggests ***M* ~ 0.2** to resolve 80% of total kinetic energy.

2.4 Time-averaged Pope criterion (2)

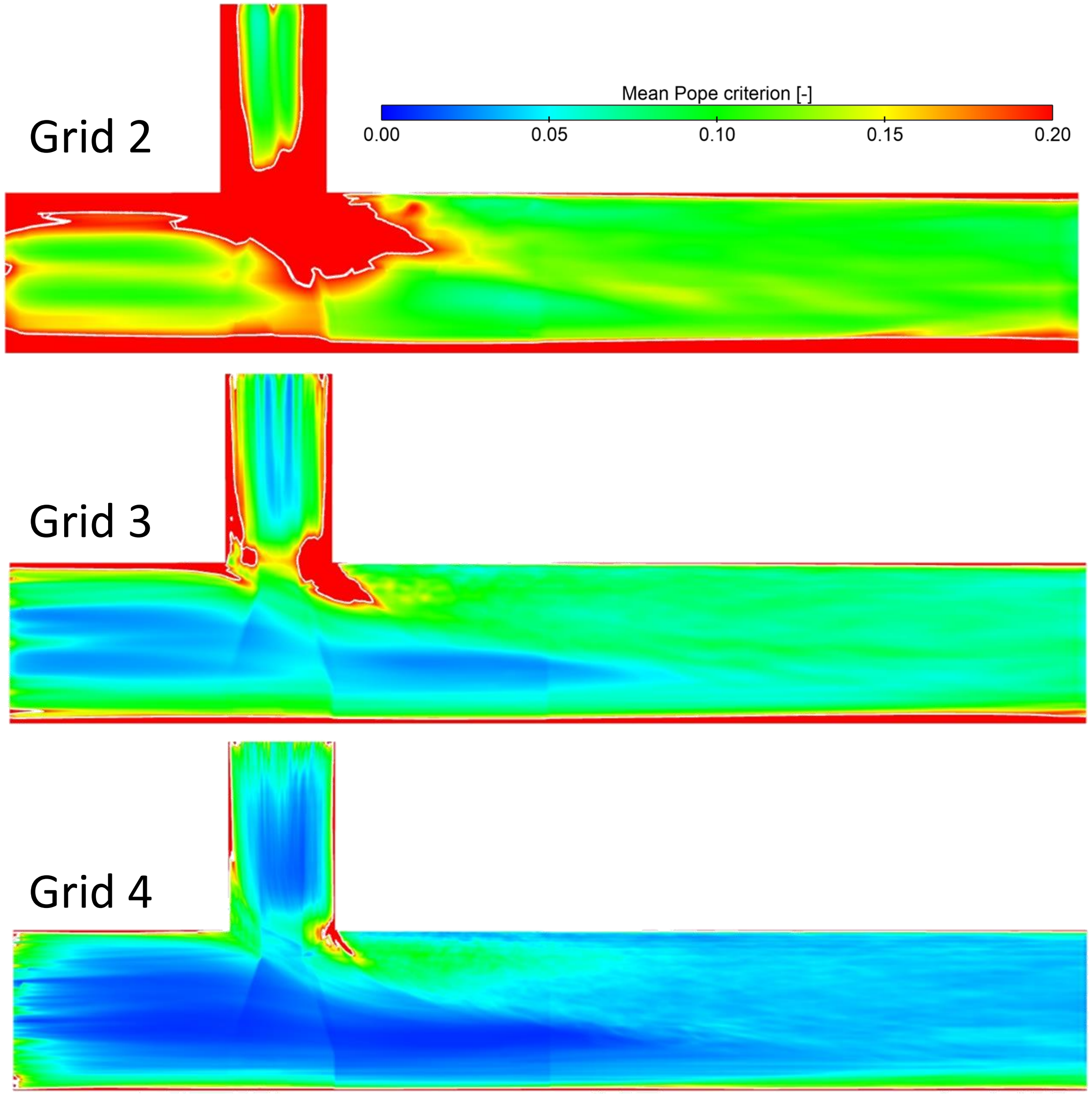

As expected, grid 1 does not show proper resolution for a Near-Wall Modeled LES as even core flow is under-resolved with M > 0.2 nearly everywhere.

Further grid refinement reduces M in the core flow but boundary layers and strong mixing region still remain under-resolved with M > 0.2 locally. It is worth pointing out that:

- Eddies get smaller near the wall with a linear dependence to normal wall-distance.
- Eddies are still highly 3D in the wall vicinity with strong anisotropic behaviour due to wall existence.

This observation confirms that LES is extremely prohibitive when one wants to capture smaller eddies in the near-wall region!

→ That is the main reason why LES is not suitable for most engineering applications with high Reynolds numbers!
→ Hybrid SRS approaches such as SBES try to alleviate this main shortcoming of LES.

2.4 Some words on a LES classification

LES classification	Resolution requirements	Pope criterion	Calculation
Wall-resolved Large-Eddy Simulation (NWR-LES)	Grid resolution is sufficient to capture 80% of energy ***everywhere***.	M < 20% everywhere.	-
Wall-modeled Large-Eddy Simulation* (WM-LES)	Grid resolution is sufficient to capture 80% of energy ***in the core flow*** *(i.e. outside the BL)*.	M < 20% away from the wall. M > 20% in wall vicinity.	4 3 2
Very-Large-Eddy Simulation (VLES)	Grid resolution is ***not*** sufficient to capture 80% of energy ***anywhere in the flow***.	M > 20% everywhere.	1

Lower cell count – faster calculation at iso-core #

Higher accuracy – slower calculation at iso-core #

*At this point, let us be careful: we use a pure LES approach here (with corresponding SGS closure as standard Smagorinsky) but grid resolution implies that a *wall-modeled LES* approach is retained. Calculations 2 to 4 are **NOT** performed with the hybrid RANS-LES approach called wall-modeled LES (WMLES)!

2.4 Time-averaged X velocity (1)

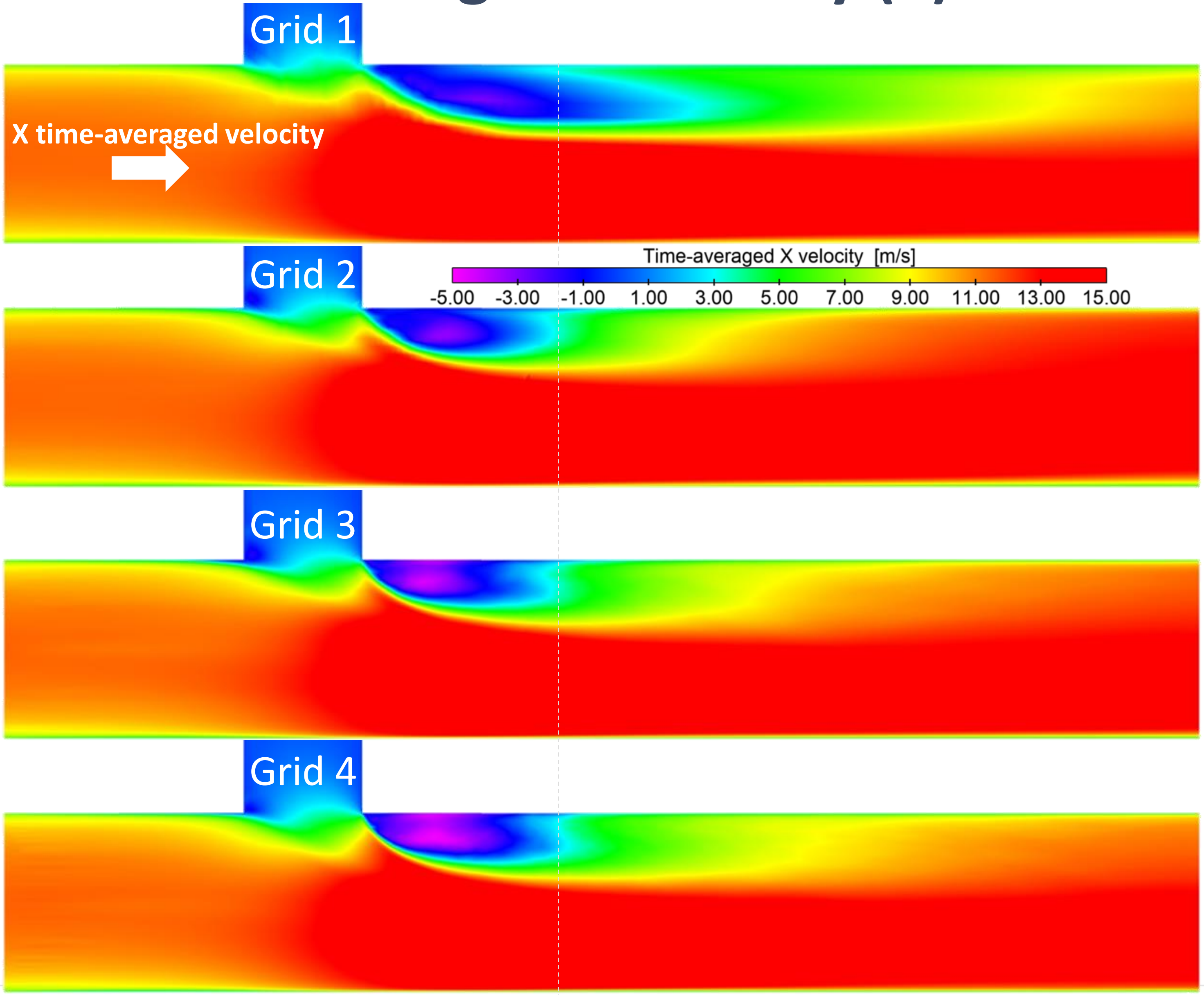

Mid-Z cut colored by the time-averaged X velocity.

Statistics for all calculations were gathered during the same duration of 1.0s, which corresponds to 5 flow-through times from inlet 1 to outlet. This duration can be considered sufficient for mean quantities (not enough for RMS though).

The time-averaged X velocity field shows that the recirculation bubble is much too long in calculation 1 compared to other calculations. It is another hint that kinetic energy is poorly redistributed between eddies here.

Calculation 3 still exhibits some changes on the shape of the flow downstream the recirculation bubble but remains very close to calculation 4, advocating for grid-independency reached at this point.

2.4 Time-averaged X velocity (2)

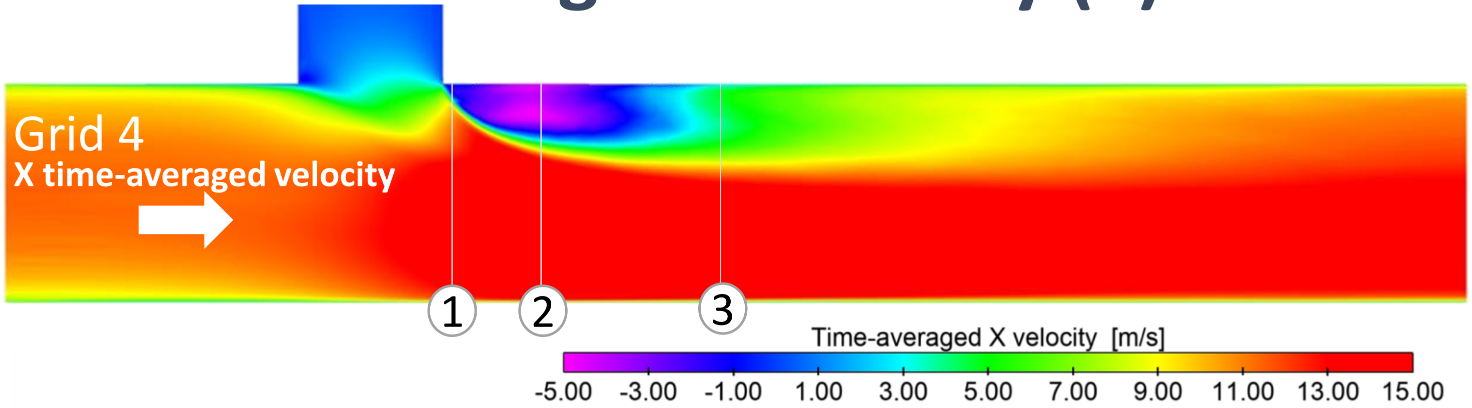

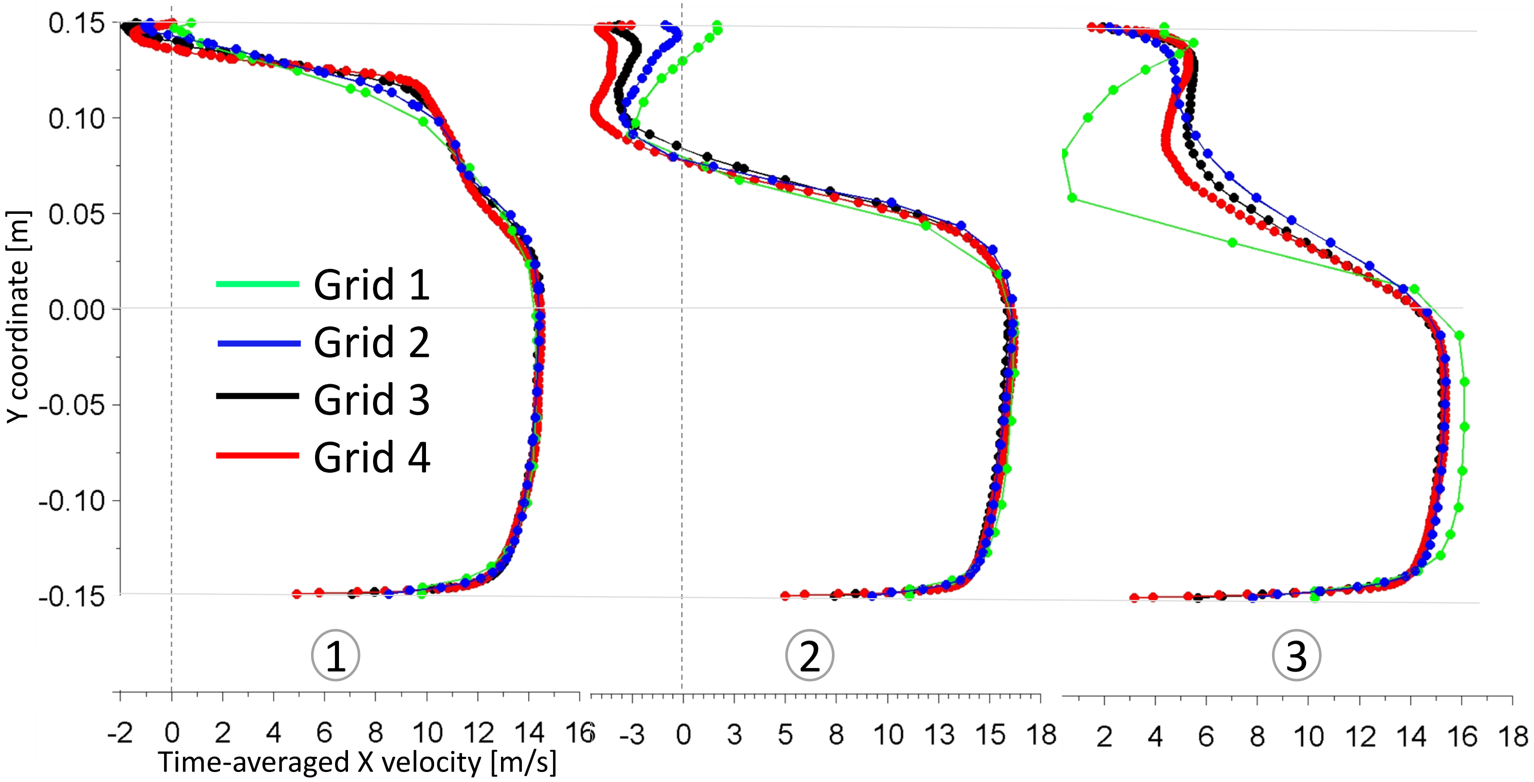

Mid-Z cut colored by the time-averaged X velocity.

Calculation 1 shows a poor definition of spatial gradient of time-averaged X velocity, especially for line 3.

→ At line 3, low grid resolution of mesh 1 results in too strong Y gradient of mean X velocity at the frontier between recirculation bubble wake and fast bulk flow. This creates less space for bulk flow to pass and artificially increases maximum X velocity in the lower part of the duct. Such effect is not observed for the finer grids.

→ For grids 2 to 4, finer grid allows to recover steeper gradient of mean X velocity.

2.4 Time-averaged Y velocity

Mid-Y cut colored by the time-averaged Y velocity.

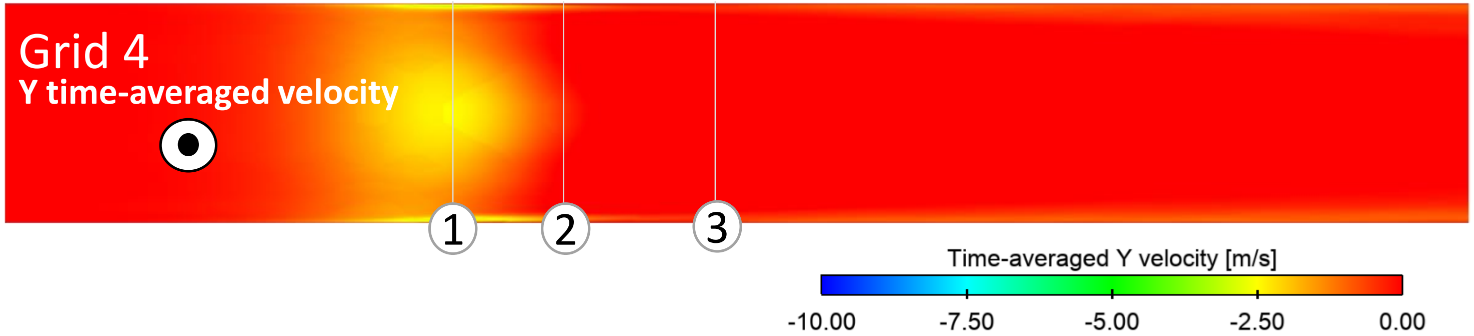

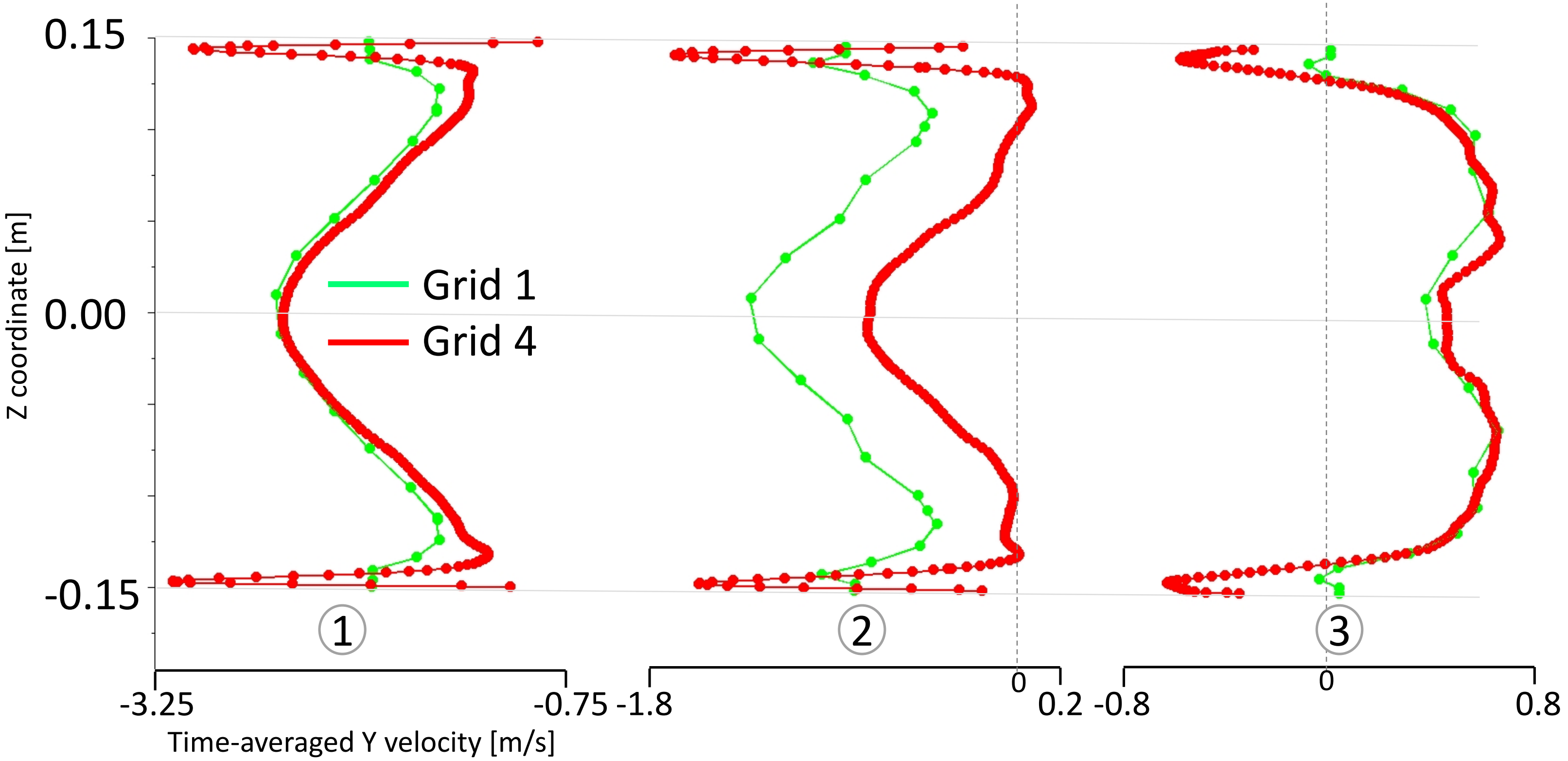

Calculation 1 exhibits lower levels of time-averaged Y velocity in the mixing region compared to calculation 4: phenomenon is particularly obvious for line 2.

Calculation 4 still needs some time-averaging when considering profile of Y velocity on lines 2 and 3: slight fluctuations are still observed.

Calculation 1 predicts highly symmetrical mean profiles but symmetry is already obtained for instantaneous fields, which is not representing correctly the turbulent unsteady nature of flow mixing here.

2.4 Time-averaged Z velocity

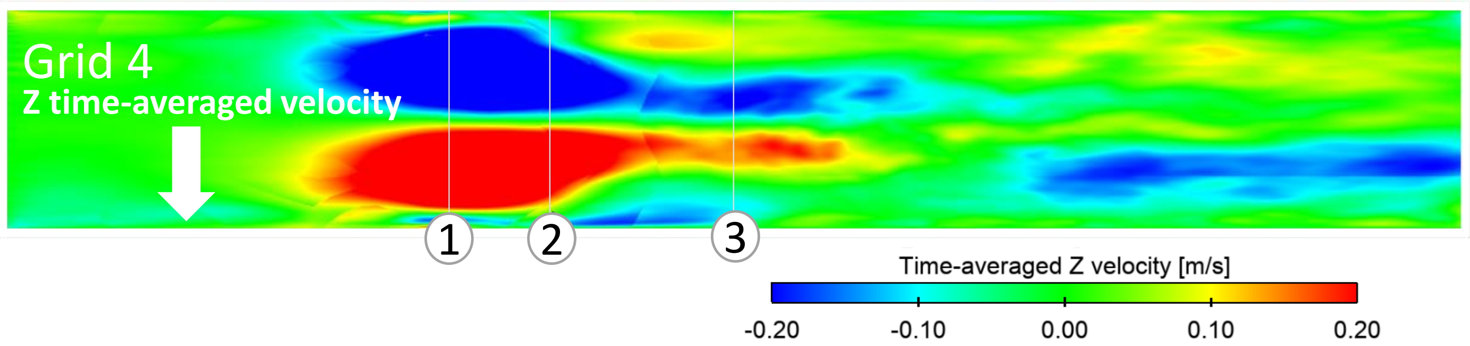

Mid-Y cut colored by the time-averaged Z velocity.

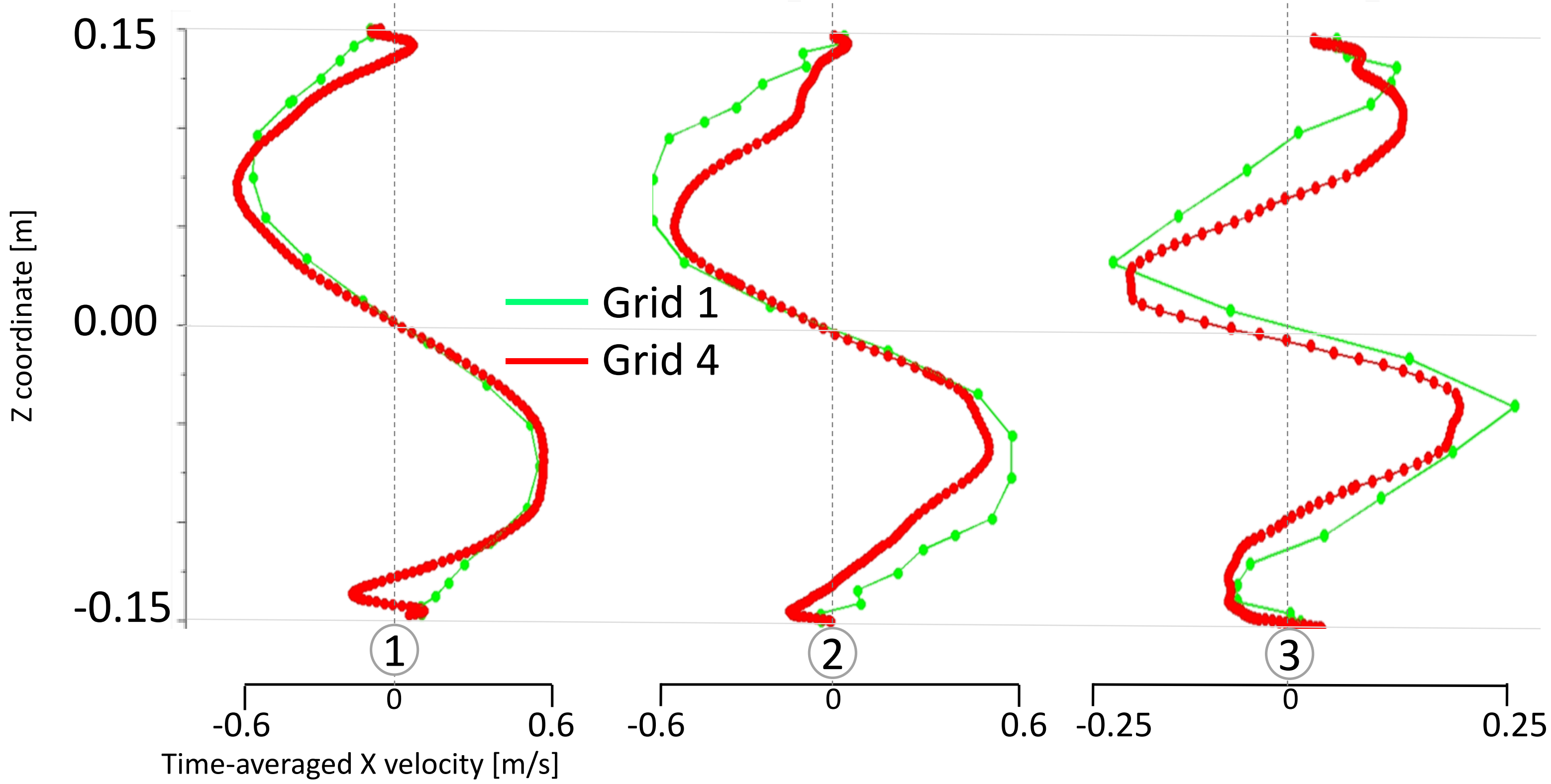

All calculations report very low values for mean Z velocity, which confirms the strong anisotropy of the mean flow field.

Grid refinement produces lower peaks of transverse velocity, particularly further downstream of the tube junction.

2.5 Total TKE Spectra – all probes

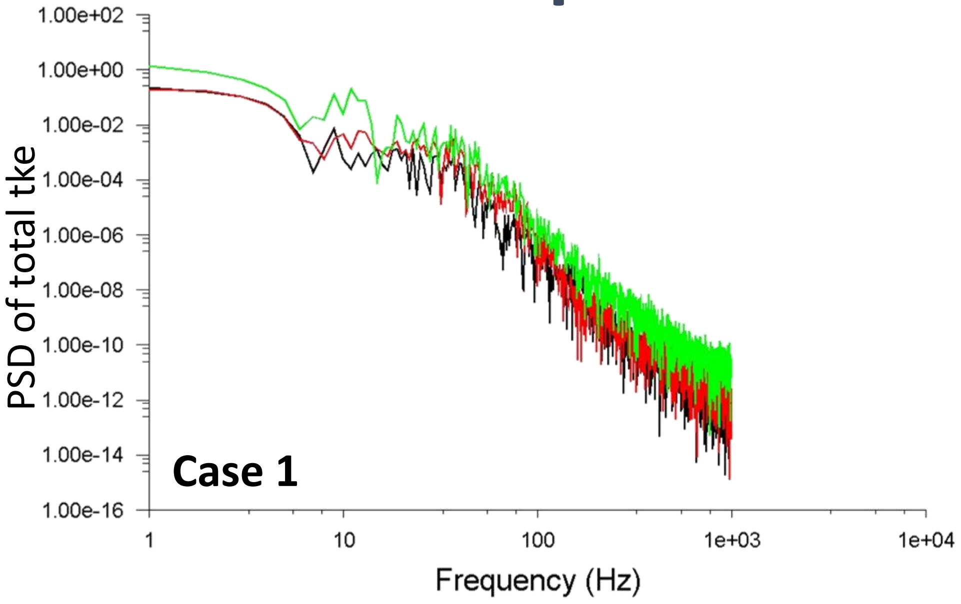

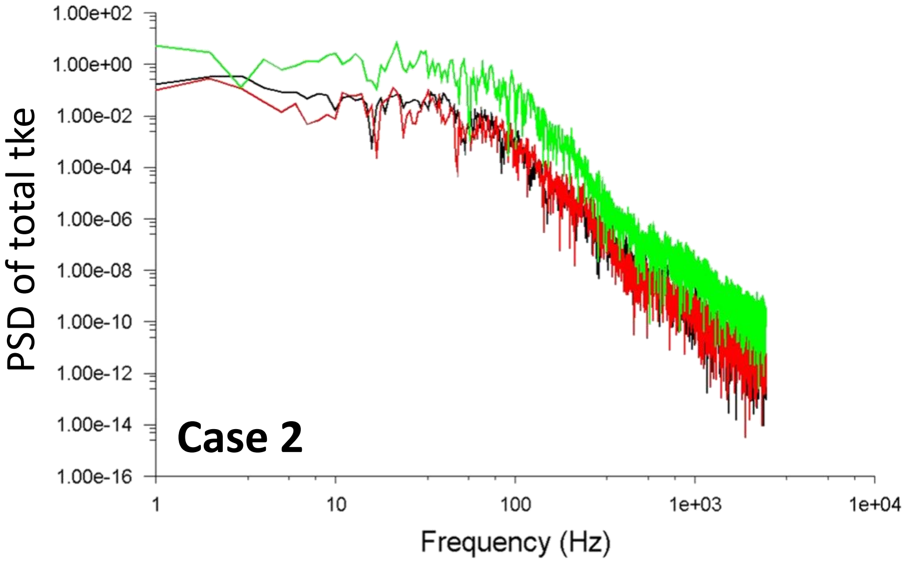

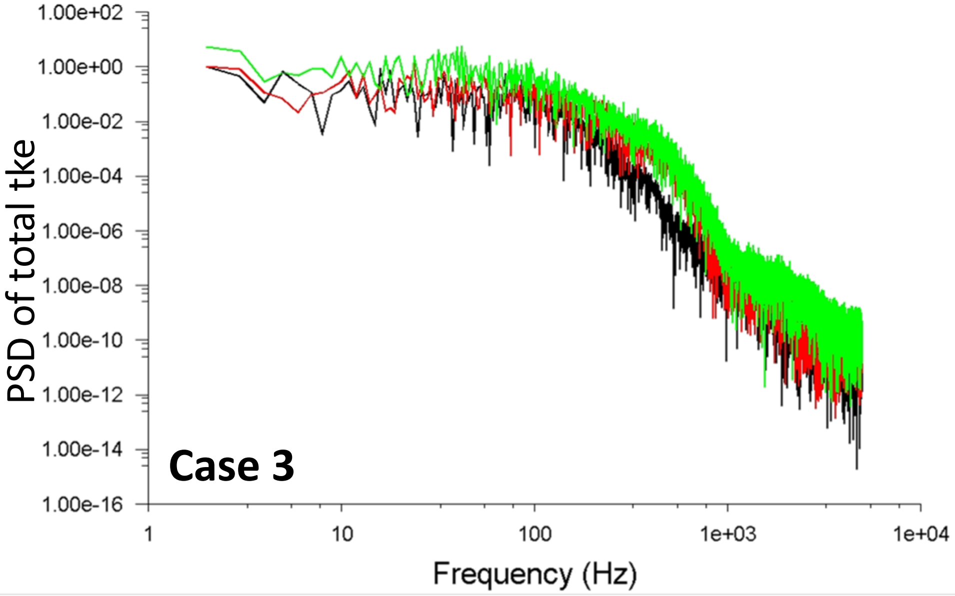

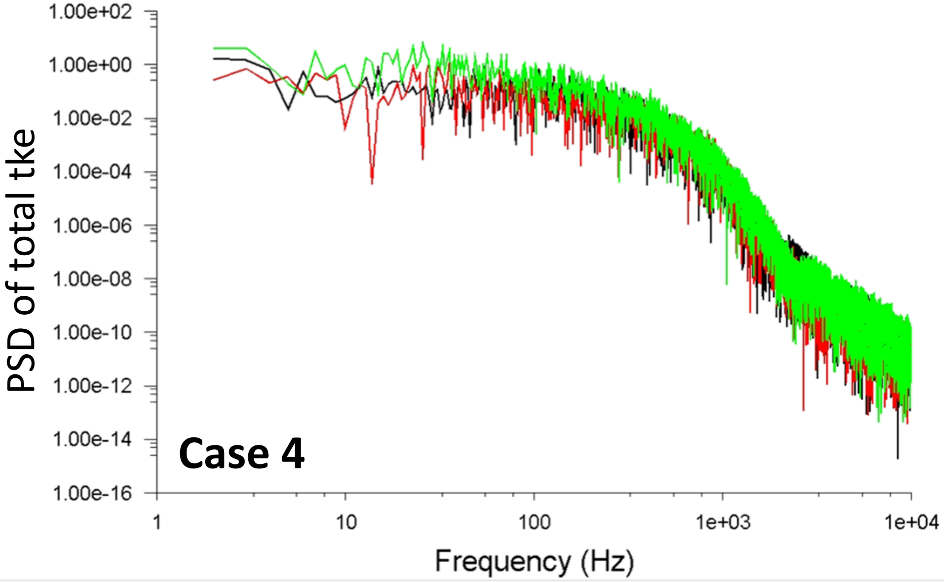

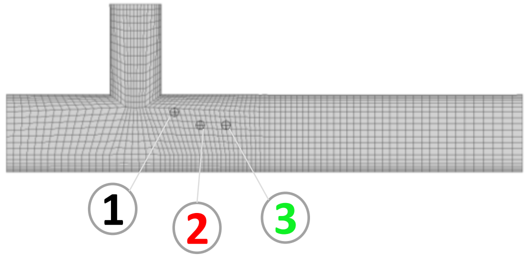

Spectra of total tke on 3 probes*:

Signal duration is the same for all calculations, so the spectral resolution is the same for all calculations.

Timestep decrease due to CFL constraint entails a higher Nyquist frequency, which explains why calculation 4 reaches 10 kHz whereas calculation 1 is restricted to 1 kHz.

**log scales considered here.*

2.5 Total TKE Spectra – probe 1

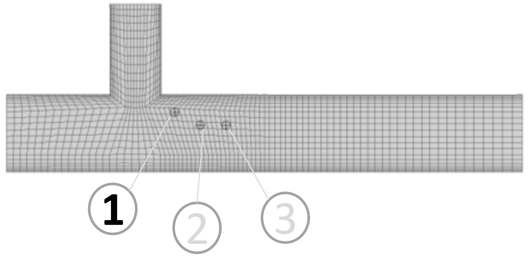

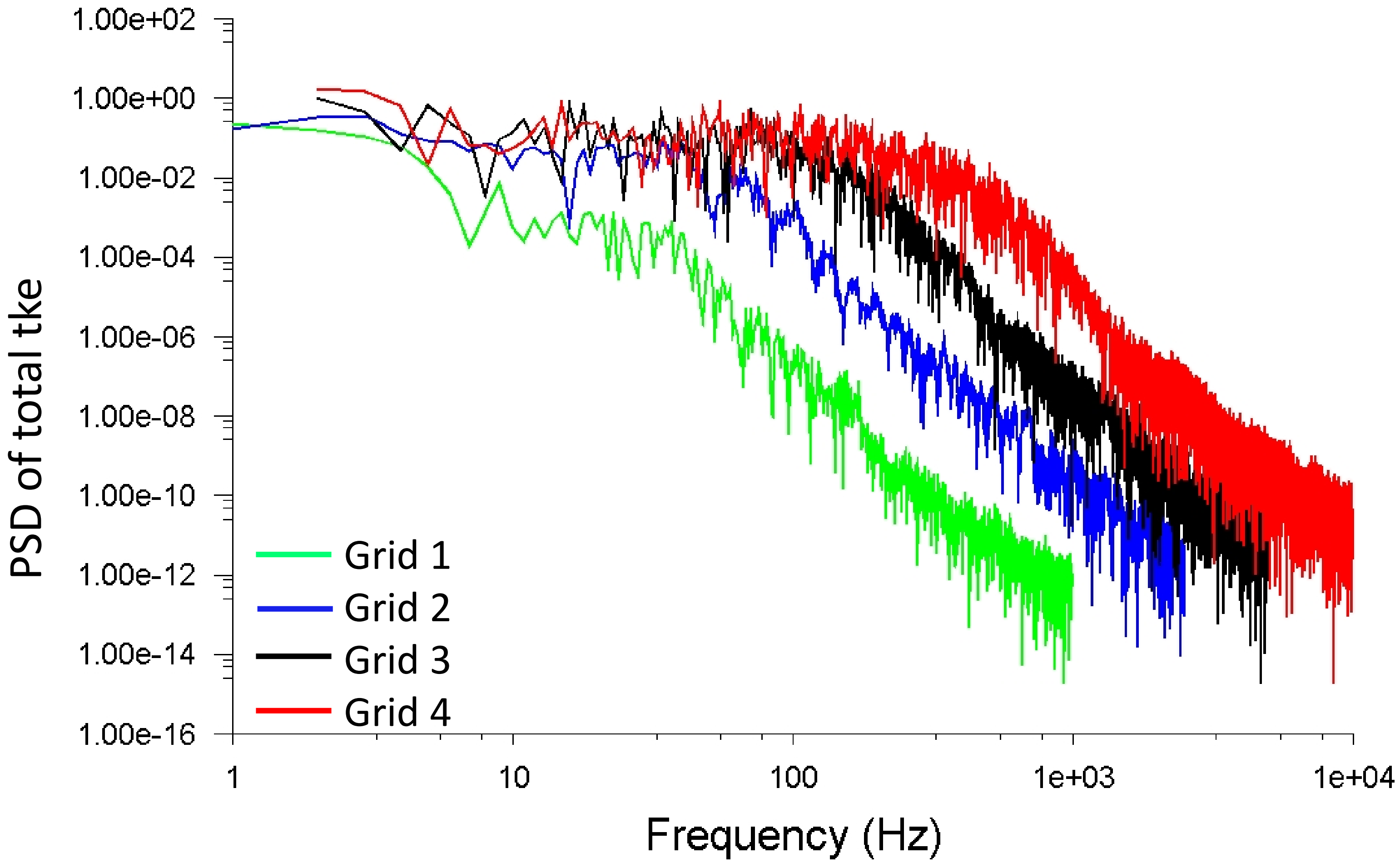

Calculation 1 does not sustain proper level of PSD for low frequencies compared to other calculations.

Regarding the trends of decay, all calculations show similar results at probe 1, probe that is located very close to corner.

Calculation 4 sustains higher PSD of total tke for lower frequencies, which indicates that a larger number of eddies create turbulent kinetic energy at lower frequencies (i.e. talking about large eddies in fact).

2.5 Total TKE Spectra – probe 3

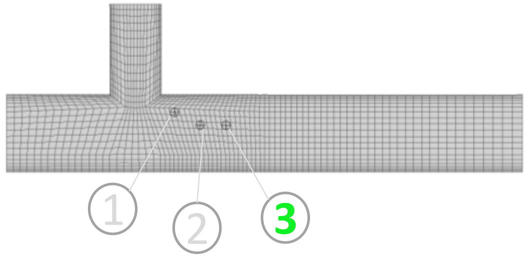

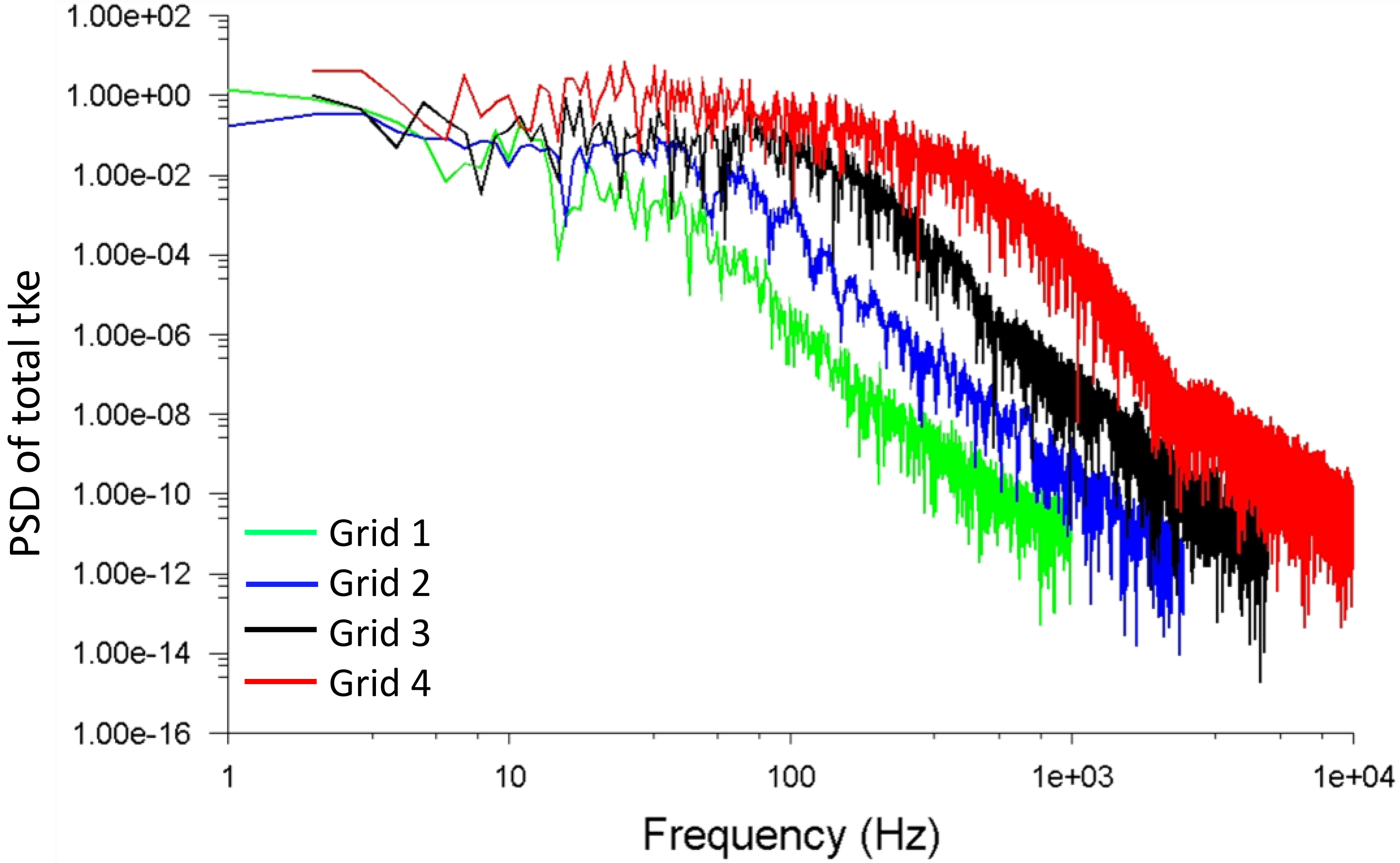

At probe 3, calculation 4 clearly shows different slopes of decay with frequency.

Some spectrum smoothing is necessary to better evaluate the slope of decay for case 4.

2.5 Total TKE Spectra – probe 3 – Calculation 4

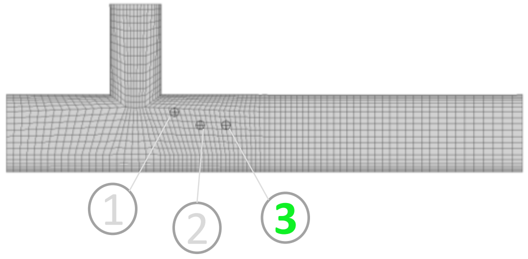

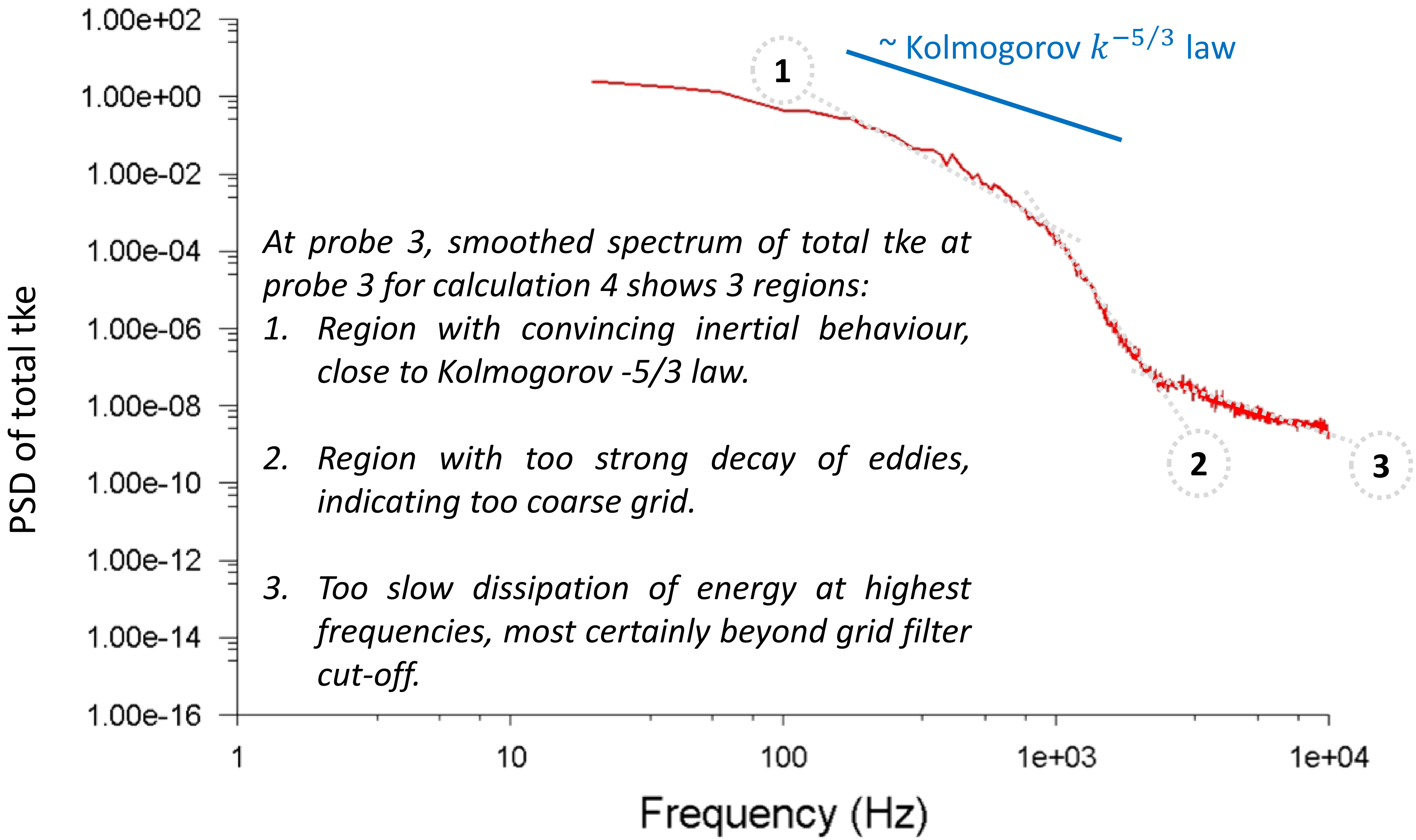

At probe 3, smoothed spectrum of total tke at probe 3 for calculation 4 shows 3 regions:

1. *Region with convincing inertial behaviour, close to Kolmogorov -5/3 law.*

2. *Region with too strong decay of eddies, indicating too coarse grid.*

3. *Too slow dissipation of energy at highest frequencies, most certainly beyond grid filter cut-off.*

2.6 Scatter plot of velocity (instantaneous vs mean) inside domain

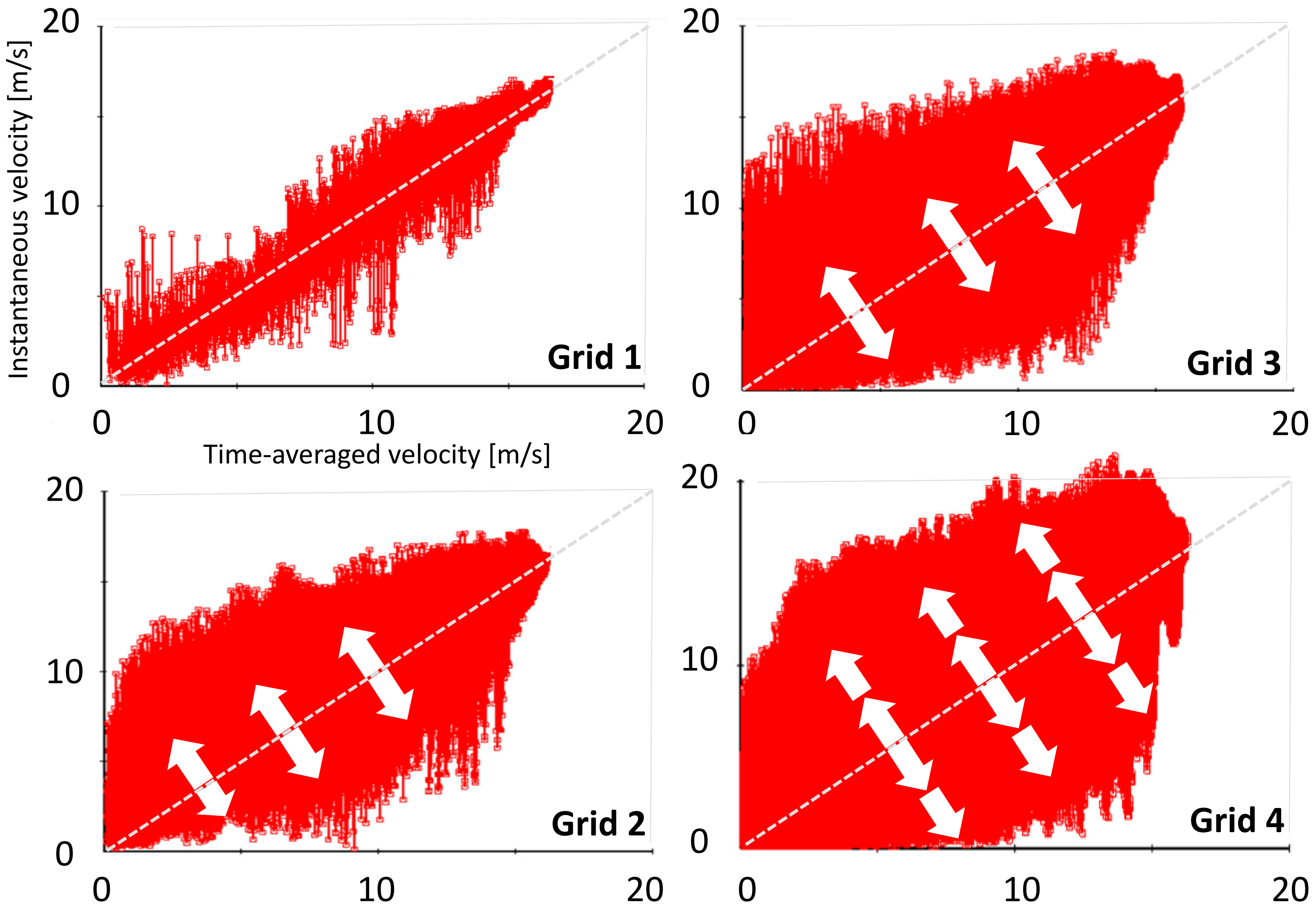

Scatter plots of instantaneous vs mean velocity inside domain show that:

- As the grid gets finer, the range of instantaneous velocities gets wider for each value of mean velocity predicted inside the domain.

- For low mean velocities, finer grids capture larger instantaneous velocities, pointing to stronger and more widely distributed flow velocity fluctuations captured compared to coarser grids.

Index

Conclusion

When globally refining grid for a LES calculation of the flow in a mixing tee, several effects were observed:

- Eddy viscosity decreased,
- Numerical* viscosity decreased,
- More eddies were captured,
- More anisotropy was observed for such eddies.

Even if refinement was applied on the whole computational domain, such effects were observed locally, involving that turbulence generation and transport occur in specific zones and are equally important to correctly represent turbulent eddies inside the flow. Sustained flow velocity gradients (i.e. the tube junction region here) then constantly feeds turbulence downstream.

The injection of vortices at inlets also benefits from a refined grid since it allows the incoming vortices to reach and excite the main turbulence generators at correct rate.

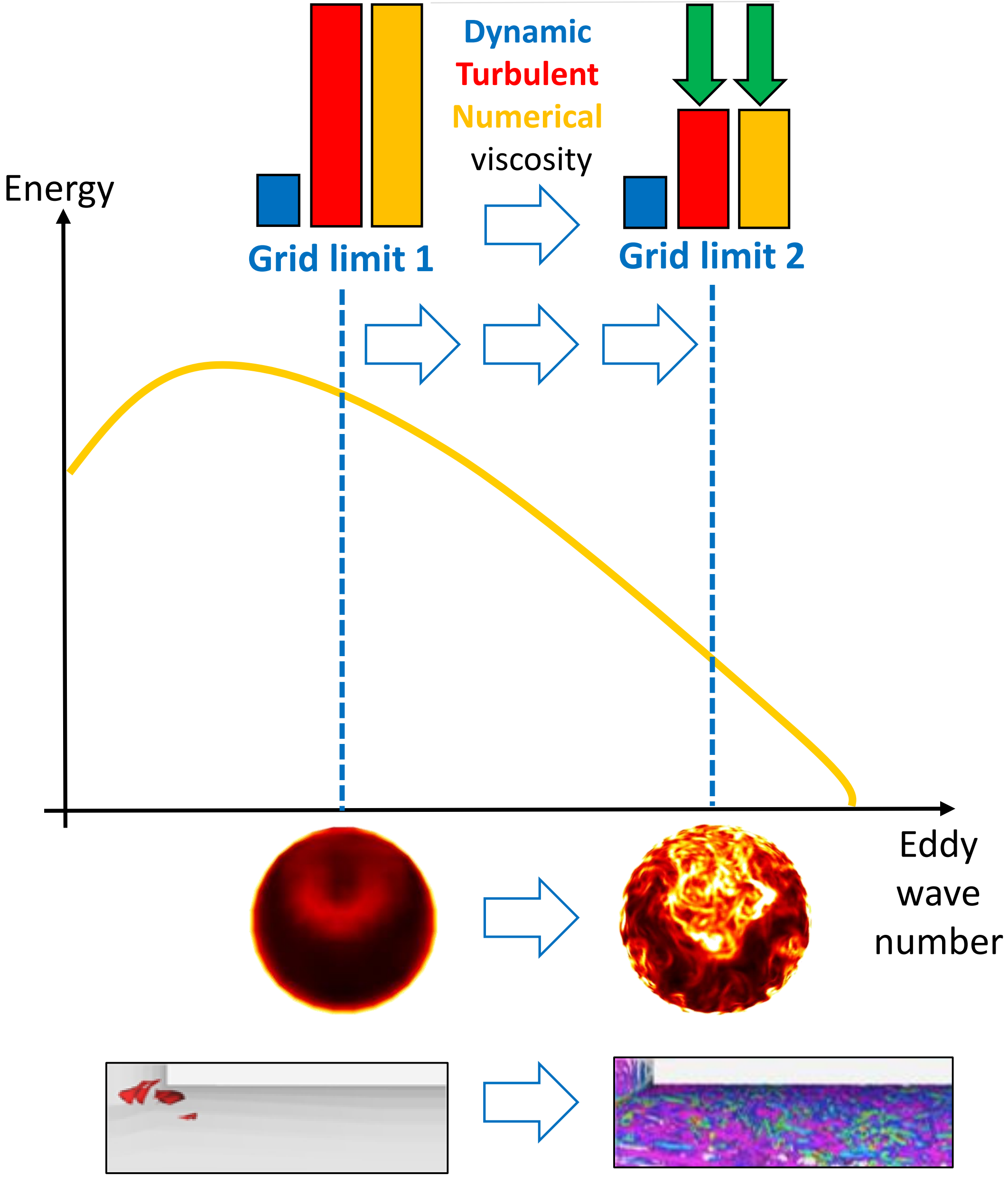

*For spatial 2nd order methods as used here on good quality hexa grids, diffusion error is prominent.

RANS vs LES?

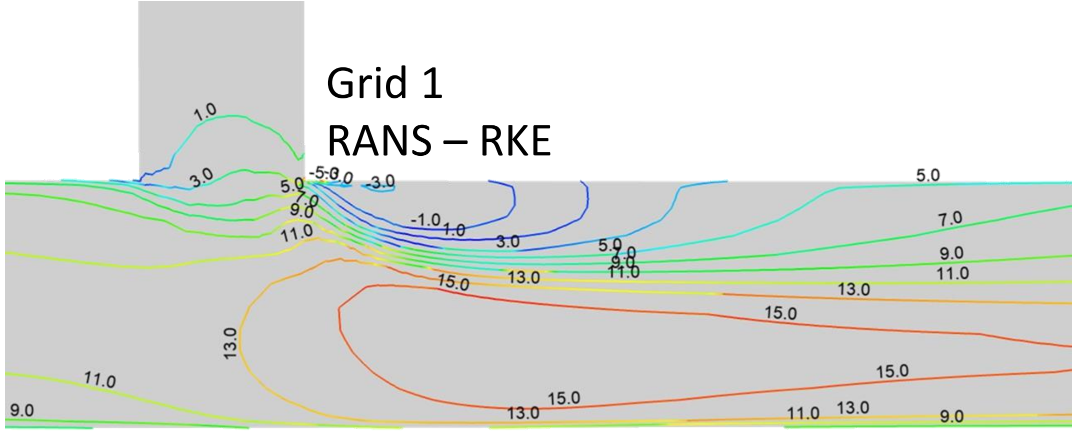

Grid 1
RANS – RKE

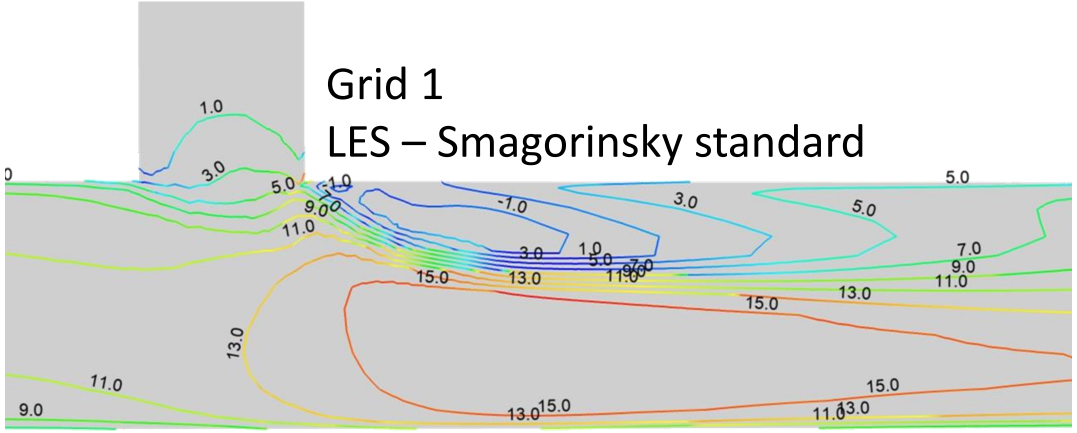

Grid 1
LES – Smagorinsky standard

→ RANS calculation can still prove very helpful as a quick *a priori* estimator for correct mesh resolution.

Mid-Z cut colored by the time-averaged X velocity.

Even on very coarse grid, steady RANS and time-averaged LES flow fields are different, particularly regarding the recirculation bubble.

This is mainly because LES involves the resolution of quantities that are random, unsteady and 3D, even if the flow is statistically homogeneous or steady. The Reynolds operator introduced in RANS involves an averaging that has other effects on these quantities.

Moreover, in LES, the stress tensor considered depends on the filter definition (spatial or spectral type, width) which can change in space and time.

RANS and LES – Grid 1

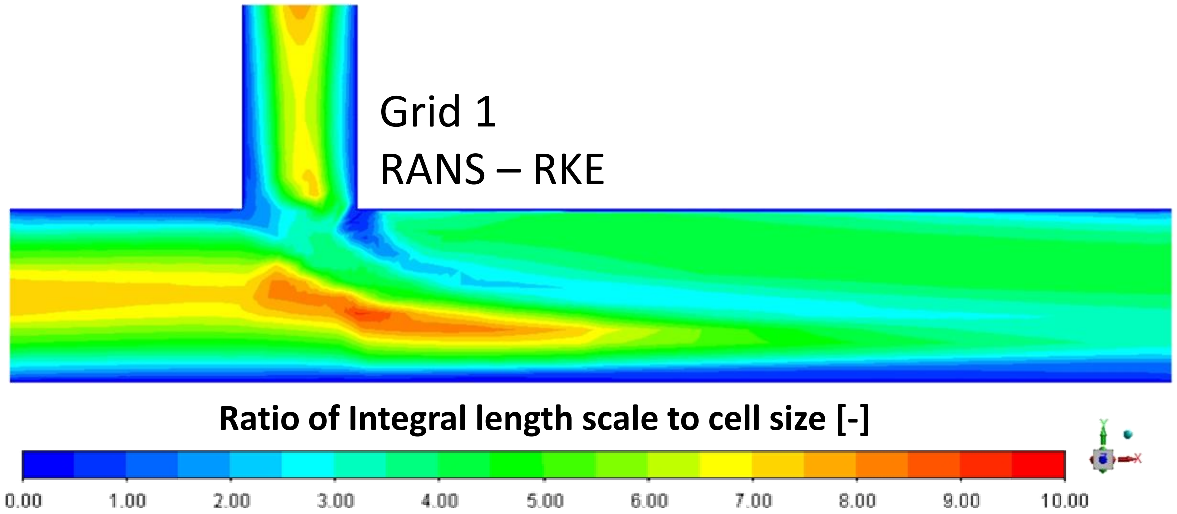

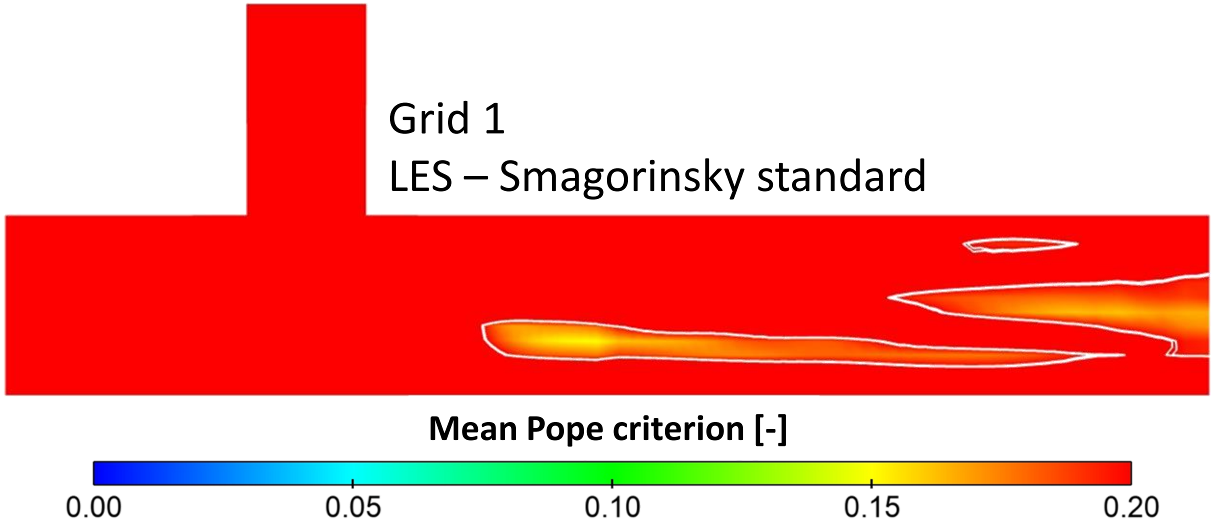

For grid 1, a ratio $\frac{l_0}{\Delta} \geq 10$ shows that at least 10 cells describe the integral length scale.

The mean Pope criterion should remain < 0.2 for 80% of total kinetic energy to be solved.

For grid 1, both markers show that a strong refinement is needed everywhere.

RANS and LES – Grid 3

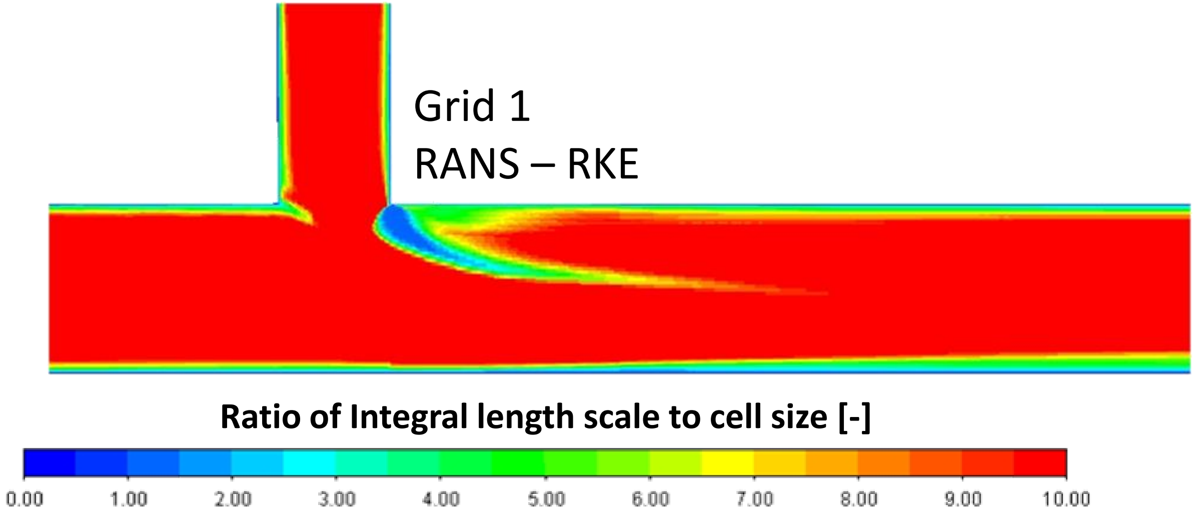

A ratio $\frac{l_0}{\Delta} \geq 10$ shows that at least 10 cells describe the integral length scale.

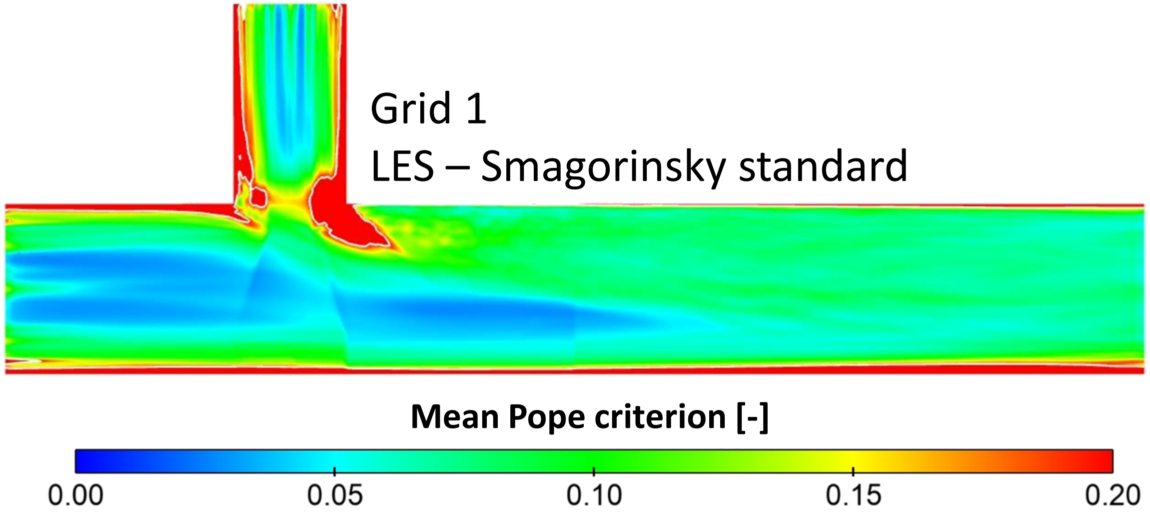

The mean Pope criterion should remain < 0.2 for 80% of total kinetic energy to be solved.

For grid 3, both markers show that some refinement is still needed for the boundary layers and at the beginning of the mixing region. This is a very satisfying observation: the LES marker obtained from RANS calculation can easily drive a relevant LES spatial resolution *a priori*!

Addenda (1) – Solutions on customer portal

Here are some additional solutions available on the ANSYS customer portal:

- Slide 6 : Solution **2039348** gives main steps for preparing LES simulation, as well as advice on main ideas/principles sustaining a great LES calculation.
  Solution **2023897** is also a nice overview of SRS LES and a mandatory reading for information on the latest hybrid SRS RANS/LES approaches developped at ANSYS.
- Slide 13 : Solution **2052121** provides an overview of eddy detection criteria available in ANSYS CFD-Post, such as the Q criterion used here.
- Slide 21 : Solution **2042805** gives more details on the Pope criterion.
- Slide 24 : Solution **2043315** gives hints on the convergence of statistics for SRS calculations.
- Slide 28 : Solution **2042949** explains how to extract spectra for total tke at probes in ANSYS Fluent.
- Slide 31 : Solution **2051343** offers an insight into spectrum smoothing within ANSYS Fluent.
- Slide 32 : Solution **2056547** shows how to draw a scatter plot in ANSYS EnSight.

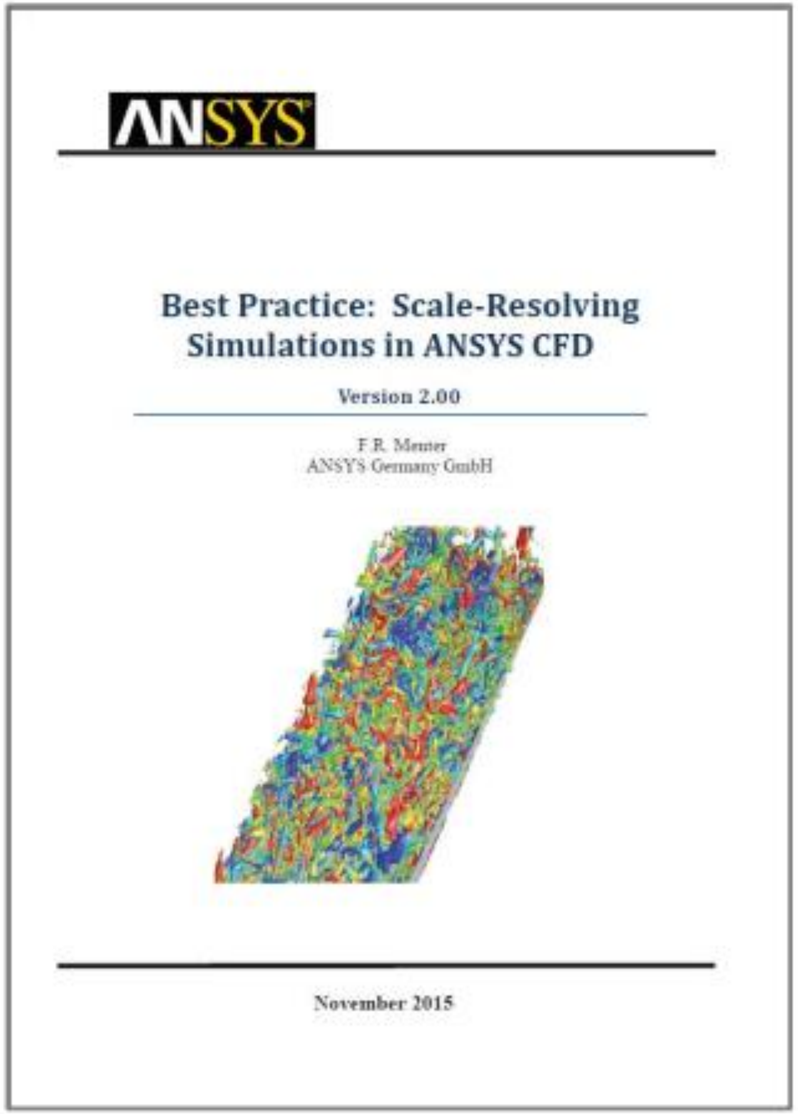
ANSYS

Best Practice: Scale-Resolving Simulations in ANSYS CFD

Version 2.00

F.R. Menter
ANSYS Germany GmbH

November 2015

Addenda (2) – Additional references on LES

Addenda (3) – Turbulence modeling within ANSYS Fluent

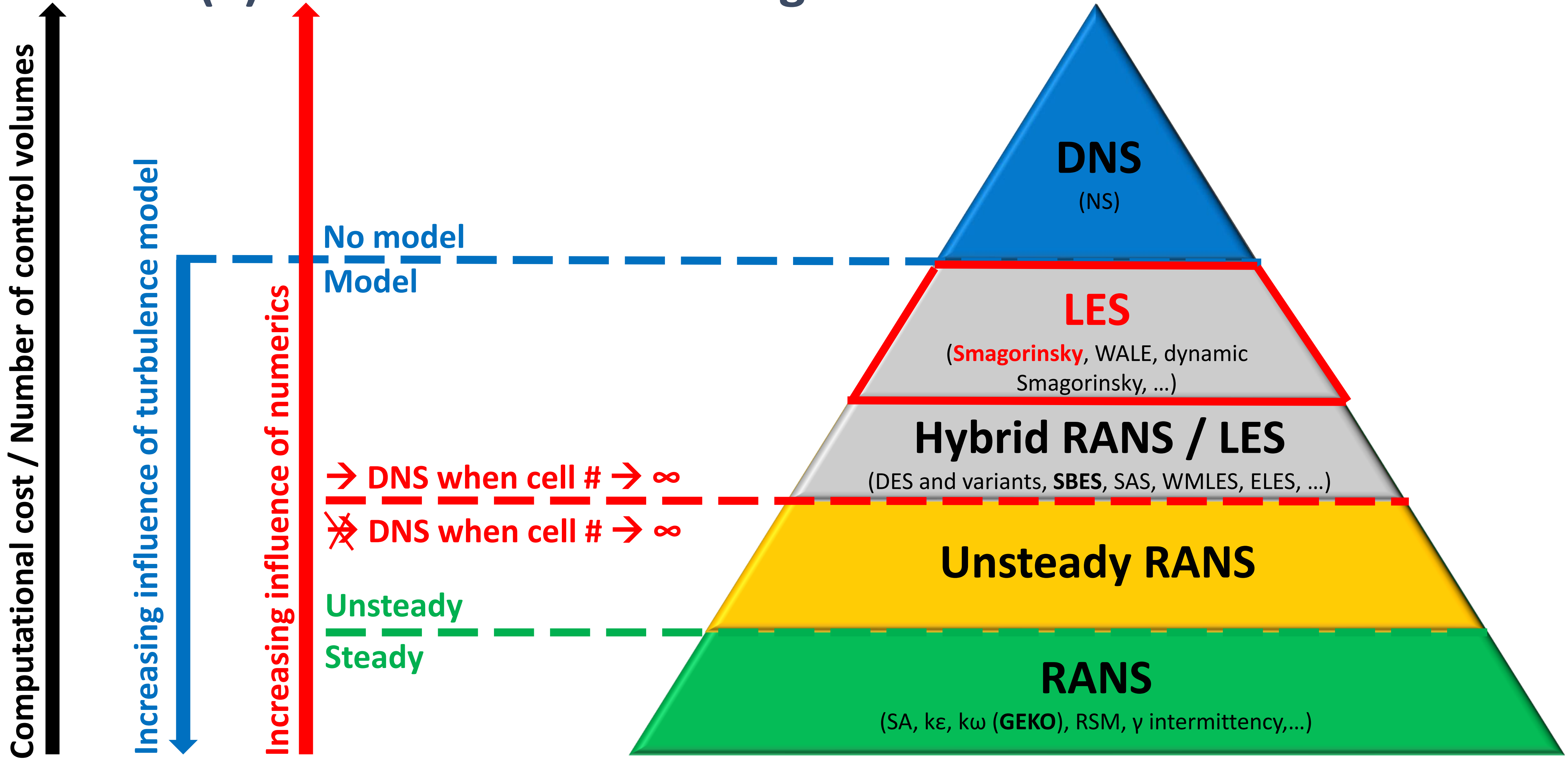

*Overview adapted from Sagaut, Deck and Terracol, 2013.